

Towards an extended taxonomy of information dynamics via Integrated Information Decomposition

Pedro A.M. Mediano^{1*}, Fernando E. Rosas^{2,3,4*}, Andrea I. Luppi^{5,6,7},
Robin L. Carhart-Harris², Daniel Bor¹, Anil K. Seth⁸, Adam B. Barrett^{8,9}

1 Department of Psychology, University of Cambridge, Cambridge, UK

2 Centre for Psychedelic Research, Imperial College London, London, UK

3 Data Science Institute, Imperial College London, London, UK

4 Centre for Complexity Science, Imperial College London, London, UK

5 University Division of Anaesthesia, University of Cambridge, Cambridge, UK

6 Department of Clinical Neurosciences, University of Cambridge, Cambridge, UK

7 Leverhulme Centre for the Future of Intelligence, University of Cambridge, Cambridge, UK

8 Sackler Center for Consciousness Science, University of Sussex, Brighton, UK

9 The Data Intensive Science Centre, University of Sussex, Brighton, UK

* These authors contributed equally to this work.

Correspondence: pam83@cam.ac.uk; f.rosas@imperial.ac.uk

Abstract

Complex systems, from the human brain to the global economy, are made of multiple elements that interact in such ways that the behaviour of the ‘whole’ often seems to be more than what is readily explainable in terms of the ‘sum of the parts.’ Our ability to understand and control these systems remains limited, one reason being that we still don’t know how best to describe – and quantify – the higher-order dynamical interactions that characterise their complexity. To address this limitation, we combine principles from the theories of Information Decomposition and Integrated Information into what we call *Integrated Information Decomposition*, or Φ ID. Φ ID provides a comprehensive framework to reason about, evaluate, and understand the information dynamics of complex multivariate systems. Φ ID reveals the existence of previously unreported modes of collective information flow, providing tools to express well-known measures of information transfer and dynamical complexity as aggregates of these modes. Via computational and empirical examples, we demonstrate that Φ ID extends our explanatory power beyond traditional causal discovery methods – with profound implications for the study of complex systems across disciplines.

Introduction

How can we best characterise the plethora of dynamical phenomena that can emerge in a system of interacting components? Progress on this question seems critical to support advances in our ability to understand, engineer, and control complex systems such as the central nervous system [1], the global climate [2], macroeconomics [3], and many others. The predominant approach for analysing such systems is in terms of cause-effect pairs, seeking to link each cause to its individual effect via a ‘causal arrow’ (see e.g. [4, 5]). However, such approaches have an important limitation that is rarely acknowledged: they neglect higher-order relationships that cannot be expressed in terms

of such arrows, which – nonetheless – have been shown to be ubiquitous in complex systems as varied as genetic networks [6], financial markets [7], baroque music [8], and the human brain [9–11].

As an alternative approach, various one-dimensional metrics have been proposed to assess the dynamical complexity of processes (e.g. [12, 13]). An interesting case of this is found in the neuroscience literature, where it has been proposed that a key feature of the neural dynamics underpinning advanced cognition, flexible behaviour, and even the presence of consciousness, can be captured by a single number that accounts for the brain’s ability to ‘integrate information.’ There have been several attempts to operationalise this notion, including the various Φ measures in Integrated Information Theory (IIT) [14–16] and Causal Density (CD) [17]; however, these measures have been shown to behave inconsistently [8, 18, 19], making empirical applications difficult to interpret.

Here we argue that the two research programs described above are limited because they are rooted in the intuition that information can only be *transferred* or *stored* between parts of a system. However, it has recently become apparent that *high-order interactions* that go beyond transfer and storage can be captured via the framework of Partial Information Decomposition (PID) [20], which demonstrates how the information that two or more sources provide about a given target can be decomposed into redundant, unique, and synergistic components [21]. Specifically, redundancy refers to information held simultaneously by both sources, unique information is that held by one source but not the other, and synergy is the information conveyed by both sources together but none of them in isolation. PID has been usefully applied to systems such as cellular automata [22, 23], artificial neural networks [24, 25], socioeconomic data [26], and gene interactions [27]. However, the information taxonomy introduced by PID is only valid in scenarios with a single target variable, being unable to discriminate between different ways in which two or more target variables can be affected collectively. This important limitation prevents PID from providing an encompassing view of the dynamics of complex systems, where the past of multiple variables affects the future of multiple variables.

In this paper we introduce the *Integrated Information Decomposition* framework (Φ ID), which combines principles from the theories of Information Decomposition and Integrated Information to overcome PID’s critical limitation and enables a complete information decomposition on groups of time series. The Φ ID framework introduces a novel information taxonomy, revealing the existence of modes of information dynamics that have not been previously reported. Furthermore, it allows us to show precisely how measures of transfer entropy and integrated information are aggregates of several qualitatively distinct modes. As proof of concept, we use two example datasets (simultaneous recordings of heart rate and respiratory volume in healthy subjects; and a neurobiologically realistic simulation of whole-brain activity) to show that the high-order effects discussed here are not merely theoretical speculations, but can have substantial effects on real-world analyses and their interpretation.

Results

Integrated information decomposition: Φ ID

Decomposing multivariate information

Consider a system composed of two interdependent elements that co-evolve over time. If the system’s future state depends only on the preceding state (i.e. if its dynamics are Markovian), then the total amount of information carried from past to future is known

as the *time-delayed mutual information*¹ [19], and can be quantified as the mutual information between past and future states of the system:

$$\text{TDMI} = I(\mathbf{X}_t; \mathbf{X}_{t+1}) = I(X_t^1, X_t^2; X_{t+1}^1, X_{t+1}^2). \quad (1)$$

Above, the superscripts 1 and 2 refer to the two elements of the system, and $\mathbf{X}_t = (X_t^1, X_t^2)$ is a shorthand notation for the system's state at time t .

One can analyse the total information flow using the *Partial Information Decomposition* (PID) framework, which decomposes the mutual information between multiple sources and a target variable into unique (**Un**), redundant (**Red**), and synergistic (**Syn**) contributions – also known as ‘information atoms’ [21]. However, just as the great strength of PID is its capacity to account for multiple sources of information, its main limitation is that it is restricted to considering only a single (potentially multivariate) target. Therefore, a direct application of PID to the TDMI would have to consider the past states of the system's elements X_t^1 and X_t^2 as sources and the joint future state of the system \mathbf{X}_{t+1} as target. Specifically, focusing on how information flows from past to future, this account decomposes the information provided by past states X_t^1 and X_t^2 about the joint future state \mathbf{X}_{t+1} , as

$$\text{TDMI} = \text{Red}(X_t^1, X_t^2; \mathbf{X}_{t+1}) + \text{Un}(X_t^1; \mathbf{X}_{t+1} | X_t^2) + \text{Un}(X_t^2; \mathbf{X}_{t+1} | X_t^1) + \text{Syn}(X_t^1, X_t^2; \mathbf{X}_{t+1}).$$

Here, the first term corresponds to the redundant information provided by both X_t^1 and X_t^2 about the joint future state of the system \mathbf{X}_{t+1} ; the second and third terms refer to the unique information that only the past state X_t^1 provides about the joint future state \mathbf{X}_{t+1} (and likewise for X_t^2); and finally, the last term accounts for the synergistic information that the two elements' past states provide about the system's joint future, only when they are considered together. Unfortunately, this approach neglects the fact that the parts of the system are distinct not only in the past, but also in the future – in other words, it can tell where the information is coming from, but not where it is going to. One naive solution would be to consider the time-reverse of the equation above, with both future states as sources and the joint past state as target (what we refer to as the ‘backwards’ PID). However, this leaves unsolved the underlying problem that PID cannot provide a unified decomposition of information across multiple sources and multiple targets simultaneously.

In order to obtain an encompassing description of the system's dynamics, one must extend the PID approach to enable multi-target information decomposition. To address this issue, our strategy is to take a temporal perspective on PID itself, focusing on how the information encoded by the PID atoms may evolve over time. For instance, information that was uniquely encoded by one element of the system in the past may become redundantly encoded by two in the future, or synergistic information may subsequently become uniquely encoded by one of the elements – and so on. This intuition suggests that when decomposing information flow between past and future in a system of two elements there are not four, but rather 16 distinct information atoms: each corresponding to a pair of the original four PID atoms evolving from past to future. Thus, we denote each Φ ID atom as a pair of PID atoms: e.g. the information that was carried redundantly in the past and becomes synergistic in the future corresponds to **Red** \rightarrow **Syn**; and the synergistic information in the past that becomes unique to X_{t+1}^1 in the future corresponds to **Syn** \rightarrow **Un**¹; and so on.

Like the original PID atoms, the Φ ID atoms are structured in a *lattice*, depicted in Fig. 1 (for a formal derivation see *Methods*). As with PID, several extra ingredients need to be specified to compute the numerical value of these atoms: in Φ ID, it can be

¹In non-Markovian systems the corresponding quantity is known as *excess entropy* [13]. Information decomposition in non-Markovian systems will be covered in a subsequent publication.

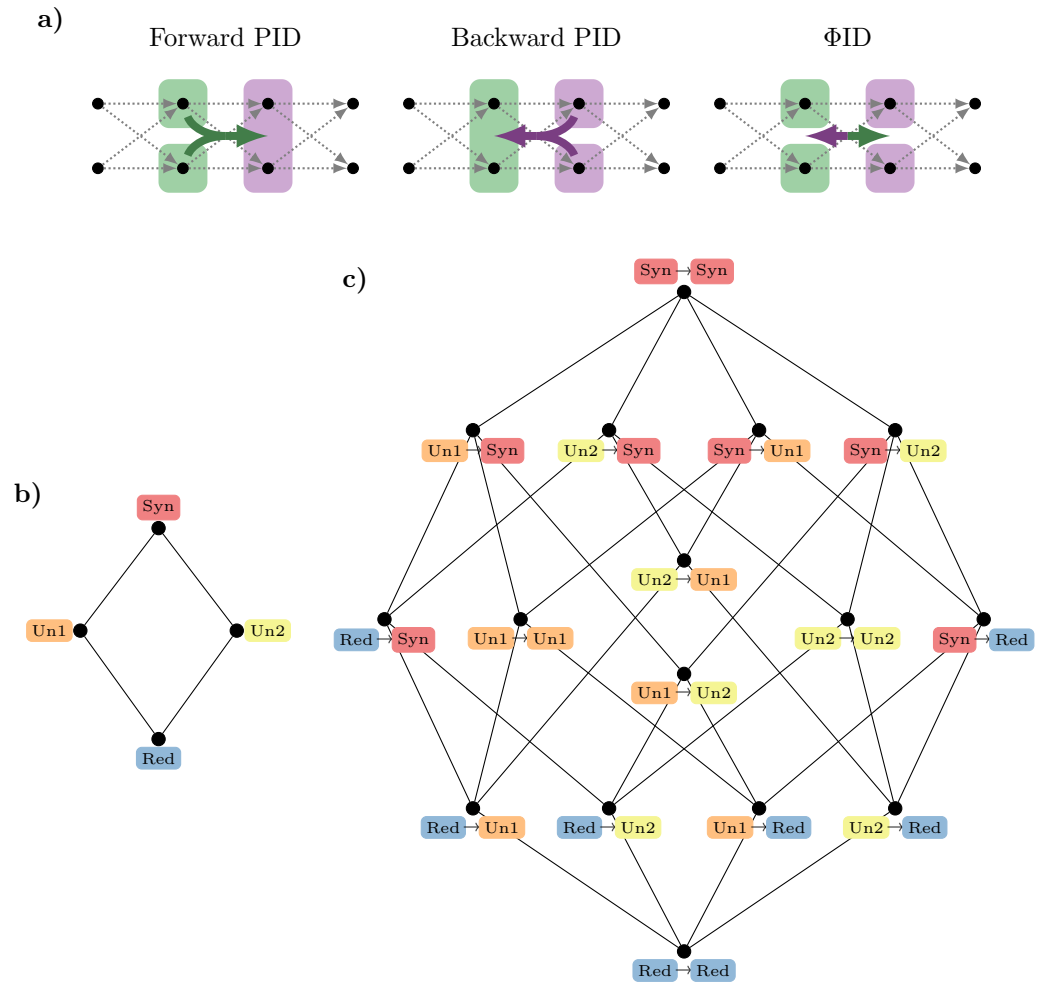


Fig 1. Lattice representation of information atoms from PID to Φ ID. **a)** System of two elements co-evolving and interacting over time, decomposed either according to a *forward PID* (left) or a *backward PID* (middle). Integrated Information Decomposition (Φ ID; right) unifies and extends both PIDs, providing an encompassing framework of information dynamics in complex systems. **b)** Redundant (**Red**), unique (**Un**) and synergistic (**Syn**) atoms in the bivariate PID lattice. **c)** Φ ID lattice for a system of two time series, where each Φ ID atom corresponds to a pair of two PID atoms that indicate how information evolves from past to future.

shown that standard Shannon theory and PID together specify a system of 15 equations for the 16 Φ ID atoms, yielding an underdetermined system. To compute the atoms one must provide one extra constraint, which can be done by introducing a *double-redundancy* function – a multi-target extension of PID’s redundancy function.² Note that the Φ ID framework does not impose a particular functional form for the double-redundancy function, and hence different functional forms can be explored. A formal development of these ideas, and its extension to systems of more than two elements, is provided in the Methods.

²For PID, it is often the redundancy function that provides the needed constraint to allow computation of numerical values for the PID atoms.

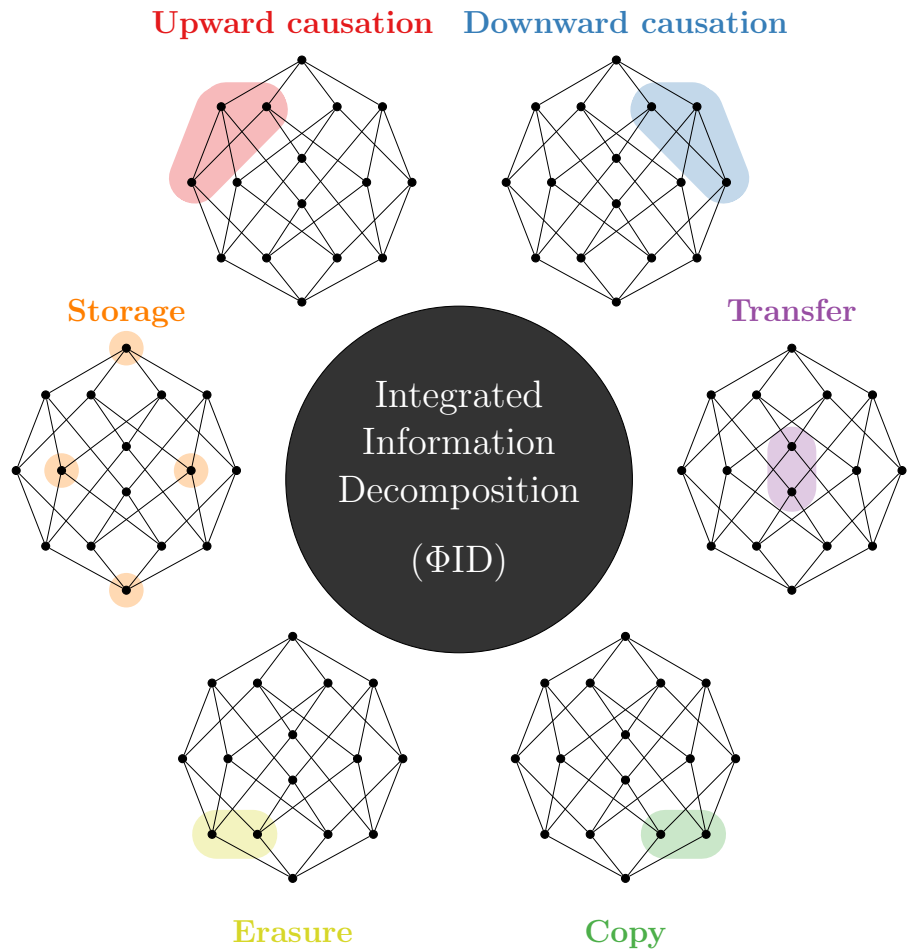


Fig 2. Taxonomy of information dynamics in complex systems. Six qualitatively different modes of information dynamics, represented in terms of their constituent atoms in the Φ ID lattice.

A new taxonomy for information dynamics in complex systems

Based on Φ ID, we propose an extended taxonomy of information dynamics according to six disjoint and qualitatively distinct phenomena (Fig. 2):

Storage : Information that remains in the same element or set of elements (even if it includes collective effect). Comprises $\text{Red} \rightarrow \text{Red}$, $\text{Un}^1 \rightarrow \text{Un}^1$, $\text{Un}^2 \rightarrow \text{Un}^2$, and $\text{Syn} \rightarrow \text{Syn}$.

Copy : Information that becomes duplicated. Comprises $\text{Un}^1 \rightarrow \text{Red}$, and $\text{Un}^2 \rightarrow \text{Red}$.

Transfer Information that moves between elements. Comprises $\text{Un}^1 \rightarrow \text{Un}^2$ and $\text{Un}^2 \rightarrow \text{Un}^1$.

Erasure Duplicated information that is pruned. Comprises $\text{Red} \rightarrow \text{Un}^1$ and $\text{Red} \rightarrow \text{Un}^2$.

Downward causation Collective properties that define individual futures. Comprises $\text{Syn} \rightarrow \text{Un}^1$, $\text{Syn} \rightarrow \text{Un}^2$, and $\text{Syn} \rightarrow \text{Red}$.

Upward causation Collective properties that are defined by individuals. Comprises $\text{Un}^1 \rightarrow \text{Syn}$, $\text{Un}^2 \rightarrow \text{Syn}$, and $\text{Red} \rightarrow \text{Syn}$.

While the downward causation mode has been discussed in the past [20], upward causation and synergistic storage ($\text{Syn} \rightarrow \text{Syn}$) have, to our knowledge, not been reported in the literature. Importantly, traditional methods of causal discovery cannot capture the type of modes that involves interactions between multiple target variables. In effect, while methods such as PID or multivariate Granger causality can effectively deal with multivariate target variables, they cannot untangle how each component of the target may be differently affected, and — more importantly — how sources may affect the target as a whole, without (or in addition to) affecting its parts. Overall, this new taxonomy leads to less ambiguous and fully quantifiable descriptions of information dynamics in complex systems, in addition to grounding abstract concepts such as upward and downward causation,³ and notions such as integrated information – as we discuss below.

A simple example of information decomposition with Φ ID

As a first example of the kind of insight that Integrated Information Decomposition can provide, let us focus on the decomposition of a variable’s so-called ‘active information storage’ (AIS) [30], which is defined as the TDMI of an individual part of the system (i.e. the mutual information between the present of one variable, X_t^1 , and its own future, X_{t+1}^1). To decompose AIS, consider that in PID the mutual information of a single source variable with the target is decomposed as the sum of redundancy (which is information that each source has about the target) and that source’s unique information. Similarly, in Φ ID AIS is decomposed in terms of redundancy and unique information, but now taking into account *both* past and future:

$$\text{AIS}(X^1) = I(X_t^1; X_{t+1}^1) = \text{Red} \rightarrow \text{Red} + \text{Red} \rightarrow \text{Un}^1 + \text{Un}^1 \rightarrow \text{Red} + \text{Un}^1 \rightarrow \text{Un}^1. \quad (2)$$

Here, $\text{Red} \rightarrow \text{Red}$ corresponds to redundant information in the past of both parts that is present in the future of both parts; $\text{Red} \rightarrow \text{Un}^1$ is the redundant information in the past that is eliminated from the second element and hence is only conserved in X_{t+1}^1 ; and similarly for the remaining atoms.

Even with this simple example, Φ ID already yields new insights into the system’s information dynamics: note that, although X_t^2, X_{t+1}^2 are not in this mutual information, $I(X_t^1; X_{t+1}^1)$ shares the $\text{Red} \rightarrow \text{Red}$ term with $I(X_t^2; X_{t+1}^2)$ by virtue of them being considered part of the same multivariate stochastic process. Therefore, if one uses simple mutual information as a measure of storage one may include information that is not stored exclusively in a given variable, resulting in a ‘double-counting’ of the $\text{Red} \rightarrow \text{Red}$ atom which can lead to paradoxical conclusions – such as the sum of individual information storages being greater than the total information flow (TDMI).

More generally, Φ ID can be used to decompose many other quantities of interest for complex systems analysis (Fig. 3), and their decompositions can help us both to understand existing measures and design new ones. In the following sections we apply this line of reasoning and the Φ ID framework to two prominent scenarios in complex systems analysis: the assessment of causal interactions between system components, and the quantification of system-wide integrated information.

Theoretical implications

Different types of integration

Measures of integrated information, usually denoted by Φ , aim to quantify the degree to which a temporal evolution of a dynamical system depends on the interdependencies

³The relation between Φ ID and causal emergence [28] can be found in a separate publication [29].

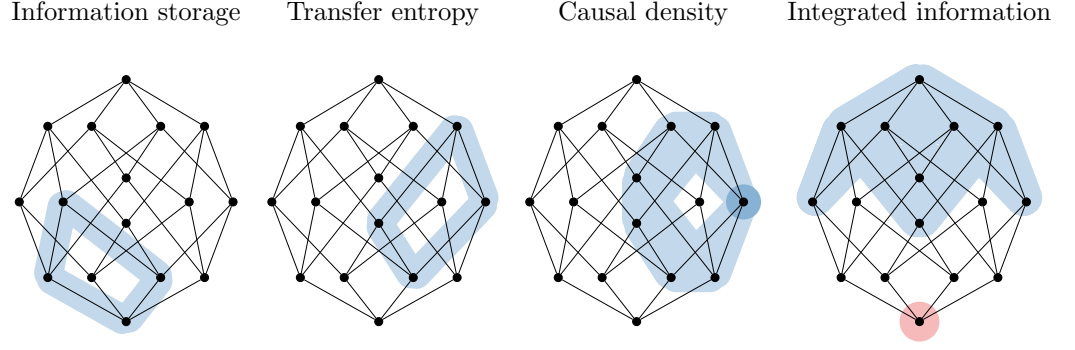


Fig 3. Common information-theoretic measures decomposed into integrated information atoms. Constituent Φ ID atoms of active information storage, transfer entropy (from X_t^1 to X_{t+1}^2), causal density (sum of transfer entropies), and whole-minus-sum integrated information, highlighted in blue. Dark blue indicates double-counting in causal density, and red indicates a negative contribution of redundancy to integrated information (see text for details).

between its parts [15],⁴ see [19] for a review. Integrated information measures have been applied widely, most notably in the neuroscience of consciousness, but also to studies of diverse complex systems [31–33]. In this section we investigate the concept of integrated information through the lens of Φ ID.

The key insight that Φ ID delivers is that there are multiple qualitatively different ways in which a multivariate dynamical process can integrate information – through different combinations of redundant, unique, and synergistic effects. To illustrate this, let’s focus on the so-called ”whole-minus-sum” empirical integrated information metric [34], which for a simple 2 component system is calculated as⁵

$$\Phi^{\text{WMS}} = I(\mathbf{X}_t; \mathbf{X}_{t+1}) - \sum_i I(X_t^i; X_{t+1}^i) . \quad (3)$$

which reflects a balance between the information contained within the whole system ($I(\mathbf{X}_t; \mathbf{X}_{t+1})$) and the information contained within the parts ($I(X_t^1; X_{t+1}^1)$ and $I(X_t^2; X_{t+1}^2)$). We apply this metric to the following elementary examples of 2 binary variables (Fig. 4):

- A **copy transfer** system, in which X_t^1, X_t^2, X_{t+1}^1 are i.i.d. fair coin flips, and $X_{t+1}^2 = X_t^1$ (i.e. the information of X_t^1 is copied to X_{t+1}^2).
- The **downward XOR**, in which X_t^1, X_t^2, X_{t+1}^2 are i.i.d. fair coin flips, and $X_{t+1}^1 \equiv X_t^1 + X_t^2 \pmod{2}$.
- The **parity-preserving random** (PPR), in which X_t^1, X_t^2 are i.i.d. fair coin flips, and $X_{t+1}^1 + X_{t+1}^2 \equiv X_t^1 + X_t^2 \pmod{2}$ (i.e. \mathbf{X}_{t+1} is a random string of the same parity as \mathbf{X}_t).

A direct calculation shows that these three systems are ‘equally integrated’: $\Phi^{\text{WMS}} = 1$ for all of them, which implies that the degree to which the dynamics of the whole cannot be perfectly predicted from the parts alone is equivalent [19, 34]. However,

⁴The parts being chosen so as to have the weakest overall informational link between them.

⁵There is only one possible partitioning of a 2 component system, so here we don’t need to search for the minimum information partition.

a more nuanced analysis using Φ ID reveals that these systems integrate information in qualitatively different ways. In effect, the integration in the copy system is entirely due to transfer dynamics ($Un^1 \rightarrow Un^2$); the downward XOR integrates information by transforming synergistic into unique information ($Syn \rightarrow Un^1$); and PPR due to information synergistic in the past and future ($Syn \rightarrow Syn$). All the other Φ ID atoms in each of these systems are zero (proofs in the Appendix).

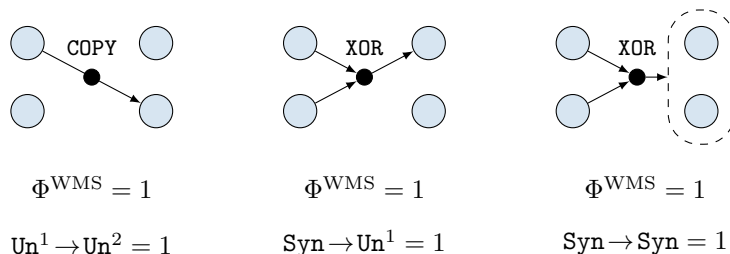


Fig 4. Example systems of logic gates. While these three systems have the same integrated information (measured with Φ^{WMS}), their information dynamics are radically different. The idiosyncrasy of each type of dynamic is captured by the Φ ID formalism, which shows that in each system there is only one non-zero atom, different for each system.

Measures of integrated information capture multiple Φ ID atoms

Within the IIT literature, researchers have proposed multiple measures aimed at quantifying to what extent a system is integrated as a whole, in terms of its parts influencing each other’s evolution over time [35]. These measures, though superficially similar, are known to behave inconsistently, for reasons that are not always clear [19]. Here we use Φ ID to dissect and compare three existing measures of integrated information (Φ^{WMS} , ψ , Φ_G) and causal density (CD), bringing to light their similarities and differences.⁶

As a systematic exploration, one can determine which measures are sensitive to which modes of information dynamics by calculating whether each measure is zero, positive, or negative for a system consisting of only one particular Φ ID atom (Table 1; proofs in the Appendix). Strikingly, each proposed measure of integration captures a distinct combination of Φ ID atoms: although generally most of them capture synergistic effects and avoid (or penalise) redundant effects, they differ substantially.

The conclusion of this analysis is that these measures are not simply different approximations of a single concept of integration, but rather they are capturing intrinsically different aspects of the system’s information dynamics. While aggregate measures like these can be empirically useful, one should keep in mind that they are measuring combinations of different effects within the system’s information dynamics. Echoing the conclusions of Ref. [19]: these measures behave differently not only in practice, but also *in principle*.

A Φ ID account of information transfer

Most methods of statistical causal discovery use the conditional mutual information⁷ as their main building block. Here we illustrate how one of such approaches, transfer entropy (TE) [4], can be decomposed in terms of Φ ID, showing that it conflates

⁶We provide definitions of each measure in the Supplementary Material – for details see Section 2.2 of Ref. [19] and the original references [15, 36, 37].

⁷Or linear variants of it, to which our conclusions also apply.

Table 1. Sensitivity of integrated information measures to Φ ID atoms. For each measure, entries indicate whether the value is positive (+), negative (-) or 0 in a system in which the given Φ ID atom is the only non-zero atom. Atom colour code taken from Fig. 1.

Φ ID atoms	Measures			
	Φ^{WMS}	Φ_G	ψ	CD
Syn \rightarrow Syn	+	0	+	0
Syn \rightarrow Un ⁱ	+	+	+	+
Syn \rightarrow Red	+	+	+	+
Un ⁱ \rightarrow Syn	+	0	0	0
Red \rightarrow Syn	+	0	0	0
Un ⁱ \rightarrow Un ⁱ	0	0	0	0
Un ⁱ \rightarrow Un ^j	+	+	0	+
Un ⁱ \rightarrow Red	0	+	0	+
Red \rightarrow Un ⁱ	0	0	0	0
Red \rightarrow Red	-	0	0	0

qualitatively distinct effects in non-straightforward ways, and fails to capture high-order modes of information flow. The TE from the system’s first to its second element, defined as $\text{TE}(1 \rightarrow 2) := I(X_t^1; X_{t+1}^2 | X_t^2)$, can be decomposed via Φ ID as

$$\text{TE}(1 \rightarrow 2) = \text{Syn} \rightarrow \text{Red} + \text{Syn} \rightarrow \text{Un}^2 + \text{Un}^1 \rightarrow \text{Red} + \text{Un}^1 \rightarrow \text{Un}^2 . \quad (4)$$

Note that, of these, $\text{Un}^1 \rightarrow \text{Un}^2$ is the only ‘genuine’ transfer term – all others correspond to redundant or synergistic effects involving both variables in past or future, which do not imply any kind of transfer phenomena. This complicates the interpretation of TE as a fully general measure of information transfer.⁸ In contrast, Φ ID can isolate the part of the transfer entropy that corresponds to information transfer through the $\text{Un}^1 \rightarrow \text{Un}^2$ term.

Additionally, Eq. (4) implies that the atom $\text{Syn} \rightarrow \text{Red}$ is accounted for in both $\text{TE}(1 \rightarrow 2)$ and $\text{TE}(2 \rightarrow 1)$. This has an important consequence: if one quantifies the total causal influence within the system via adding up both TEs (a quantity known as *unnormalised causal density* (uCD) [19]), this may overestimate the effective interdependencies by double-counting this atom (Fig. 3). In fact, the double-counting of $\text{Syn} \rightarrow \text{Red}$ implies that uCD can potentially be even larger than TDMI. While this overestimation of uCD has been noted before [37], Φ ID not only reveals the precise reason for this overestimation, but also provides a practical solution: one can correct uCD by subtracting the double-counted Φ ID atom. This problem – and its solution – may have important consequences in fields such as computational neuroscience, where the total TE of a brain region is a popular metric of its relevance for the brain’s hierarchical organization [11, 38].

The decomposition of uCD via Φ ID reveals another important limitation of traditional causal discovery methods: they do not account for modes of information flow

⁸Similar concerns about TE have been raised in Ref. [20].

that involve synergy in the targets. Therefore, while these methods account for possible interactions of source variables, they neglect interactions in the targets – which are never considered jointly. As an example, take the parity-preserving system in Fig. 4: this system has zero CD and zero AIS, yet it clearly has dynamical structure (as picked up by Φ^{WMS}). This is an example of information being carried purely in high-order effects, in a way that common measures like AIS and TE are unable to capture. More generally, we expect this to be particularly prevalent in systems with distinct micro- and macro-scale behaviour [28, 29].

Numerical examples

In this section we showcase three applications of ΦID to simulated and real data, illustrating the capabilities of ΦID to yield new insights and solve practical problems. As stated above, the numerical calculation of ΦID atoms depends on a choice of double-redundancy function – which, as in the case of PID, gives room to a range of options (see e.g. Refs [21, 39–41]). In all examples below we use a multi-target extension of the Common Change in Surprisal (CCS) measure by Ince [39]; furthermore, we show that our all the results replicate with a multi-target extension of Barrett’s Minimum Mutual Information (MMI) measure [40] (see Supplementary Material).

Why whole-minus-sum Φ can be negative

ΦID can be further leveraged to explain certain behaviours of integrated information and dynamical complexity measures. In particular, Φ^{WMS} can sometimes take negative values, which could suggest a counter-intuitive notion of a ‘negatively integrated’ system. In fact, this behaviour has been used as an argument to discard Φ^{WMS} as a suitable measure of integrated information [36, 37]. ΦID can provide an explanation of this otherwise paradoxical behaviour, and furnishes a simple solution.

By applying ΦID to the definition of Φ^{WMS} in Eq. (3), one finds that Φ^{WMS} accounts for all the synergies in the system, the unique information transferred between parts of the system and, importantly, the negative of the **Red**→**Red** atom (Fig. 3; see Supplementary Material for details). The presence of this negative double-redundancy term shows that Φ^{WMS} can be negative in highly redundant systems, in which **Red**→**Red** is larger than all other atoms that constitute Φ^{WMS} . This is akin to Williams and Beer’s [21] explanation of the negativity of the interaction information [42], applied to multivariate processes. Based on this insight, one can formulate a ‘revised’ measure of integrated information, Φ^{R} , by adding back the double-redundancy, which includes only synergistic and unique transfer terms.

We computed Φ^{R} numerically for a simple two-node autoregressive (AR) system, mimicking the setting in Ref. [19]. The system consists of two continuous variables with dynamics such that $\mathbf{X}_{t+1} \sim \mathcal{N}(A\mathbf{X}_t; \Sigma)$, with A being a 2×2 matrix with all entries set to 0.4, and Σ a noise (or *innovations*) covariance matrix with 1’s along the diagonal and a given noise correlation (c in the notation of Ref. [19]) in the off-diagonal entries. We calculated Φ^{WMS} and Φ^{R} with respect to the system’s stationary distribution, which can be shown to be a multivariate Gaussian. Plots of both quantities are shown in Fig. 5, and details of the computation can be found in the Appendix.

As expected, Φ^{WMS} drops below zero as synergy decreases and redundancy increases with noise correlation. However, after adding back the double-redundancy term, the revised version, Φ^{R} , tends to 0 for high noise correlation, which is more consistent with some of the other measures highlighted in Ref. [19], e.g. CD and Φ^* .

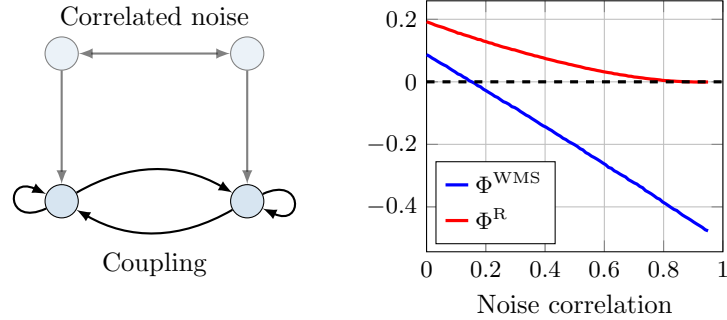


Fig 5. Standard and revised Φ^{WMS} in a two-component noisy autoregressive system. As the noise injected to both components becomes more correlated, Φ^{WMS} drops below zero while Φ^{R} remains positive.

Information decomposition in simulated whole-brain activity

We next analysed simulated whole-brain activity via the well-known Dynamic Mean Field (DMF) model introduced by Deco *et al.* [43]. This model represents cortical regions as macroscopic neural fields, whose local dynamics are described by a set of coupled differential equations. The DMF model incorporates realistic aspects of neurophysiology such as synaptic dynamics and membrane potential [44–46], and is informed by a network of anatomical connections obtained e.g. from diffusion tensor imaging (DTI) - while having the advantage of being free from physiological noise confounds. An additional biophysical haemodynamic model [47] enables the firing rates generated by the DMF model to be transformed into BOLD signals similar to resting-state fMRI data from humans, and that have been subject of study in applications of the DMF to model the neural effects of sleep [48], anaesthesia [49], and psychedelic drugs [50].

We simulate the DMF equations using a DTI-based connectome obtained from the public Human Connectome Project data [51] using the same model settings as Herzog *et al.* [50], and compute Φ^{WMS} and Φ^{R} for all pairs of brain regions.⁹ These values were calculated for varying values of a global coupling parameter (denoted by G) and the resulting average values (over all pairs of brain regions) were then analysed. The details of the model, the simulation procedure, and the computation of integrated information measures can be found in the Appendix.

As shown in Fig. 6, for values of G close to 2 the mean firing rate of the model increases sharply, reminiscent of a phase transition. At this point Φ^{WMS} shows a marked decrease, suggesting that the system is least integrated in the transition region. In fact, the value of Φ^{WMS} is often less than zero, which would correspond to the conceptually problematic notion of a system that is ‘negatively integrated.’ Crucially, however, when the double-counting of redundancy is corrected and Φ^{R} is used instead, a completely different picture appears: integration (understood as synergy plus transfer) is always positive, and it strongly *increases* and peaks in the transition region. This result aligns well with prior literature [50, 52] showing that the point $G = 2$ corresponds to the model’s optimal fit to data from awake subjects, and that a high level of integration is required for the normal operation of the brain in healthy, conscious individuals [14].

The strong discrepancy between Φ^{WMS} and Φ^{R} confirms that the concerns regarding the conflation of multiple information effects highlighted throughout this article are not a mere theoretical issue, but can trigger misleading interpretations in the analysis of

⁹The choice of analysing pairs of regions is only for convenience, as the theory is defined to systems of any size.

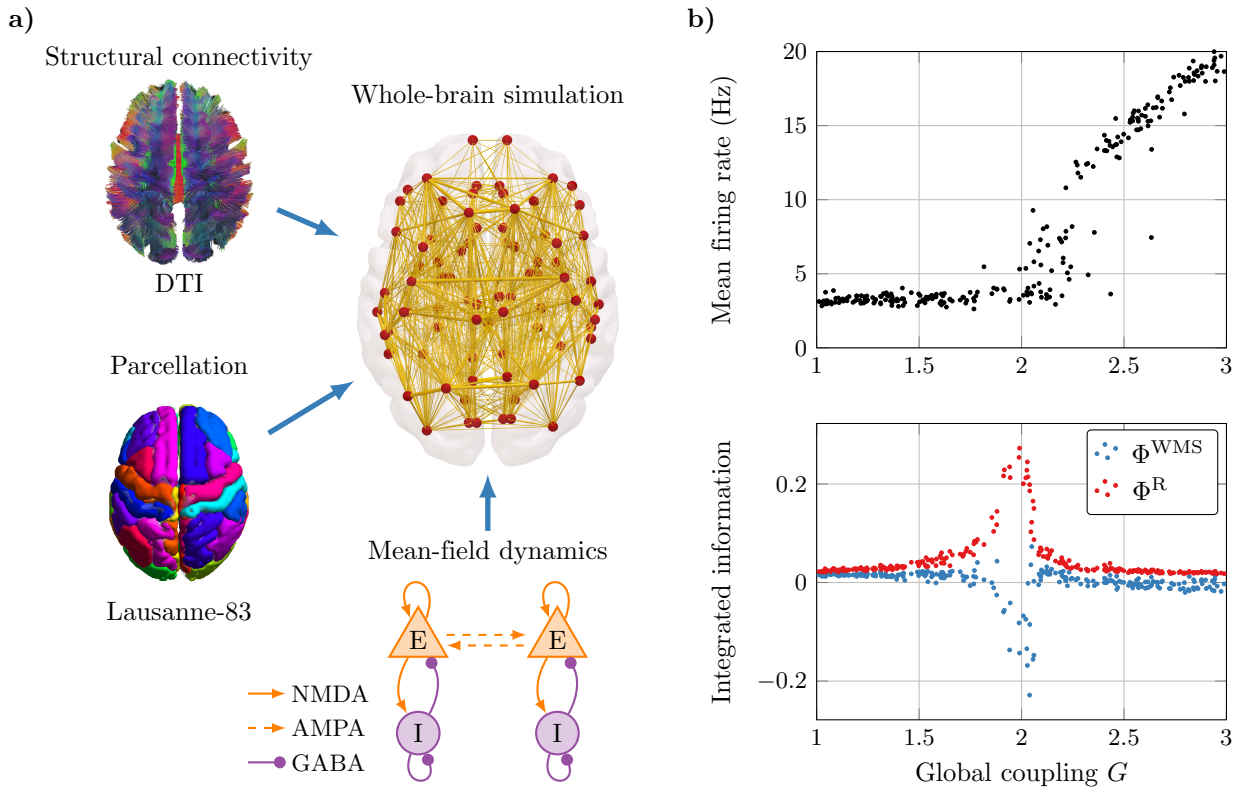


Fig 6. Measures of integrated information in a whole-brain computational model. a) Schematic diagram of the Dynamic Mean-Field (DMF) model [43,49], which combines a DTI-based connectome and a whole-brain parcellation to simulate realistic BOLD signals. b) As the global coupling parameter G is increased, the mean firing rate exhibits a sharp increase at approximately $G = 2$. Importantly, Φ^{WMS} shows a downward peak, suggesting a conceptually problematic negative value of integration – while the revised measure Φ^R shows a strong positive peak.

neuroscientific data. Hence, this example illustrates the capability of ΦID to disambiguate between qualitatively different dynamical phenomena in time series data.

ΦID sheds new light on empirical results

To provide an empirical demonstration of the capabilities of ΦID , we used it to study the dynamical relationship that exists between heart rate and respiration in healthy human subjects. This choice was motivated by the well-known influence of respiration on heart rate, which can be captured in terms of transfer entropy between respiratory volume and heart rate time series [53–55]. Therefore, we sought to investigate how the ΦID framework could be used to decompose this effect into its constituent informational elements.

For this purpose, we analysed the Fantasia database [56], an openly available dataset that contains data from 40 healthy subjects while watching the Disney movie ‘Fantasia.’ Following the preprocessing pipeline outlined in Ref. [53], we extracted synchronised time series for inter-beat intervals from the ECG timeseries, and detrended the respiratory volume. Using the resulting data, we calculated both the transfer entropy from heart to breath and from breath to heart, and then proceeded to decompose these quantities in terms of their ΦID constituents (Fig. 7).

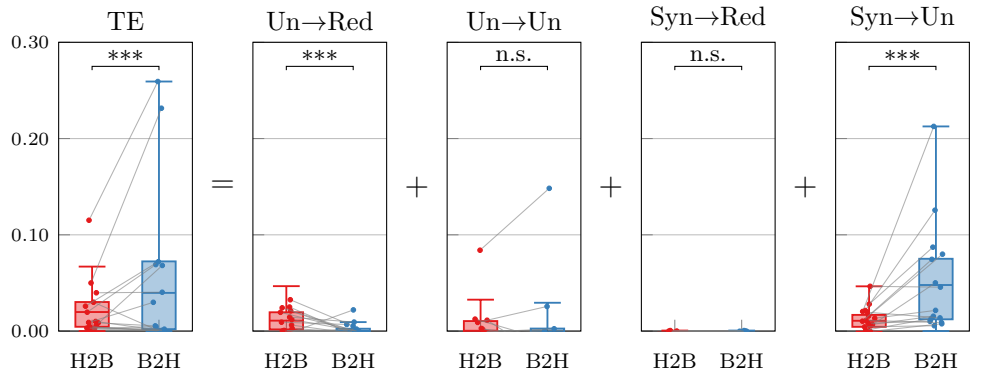


Fig 7. Decomposition of information transfer between heart rate and respiratory volume. Transfer entropy decomposed into its four constituent Φ ID atoms, calculated in both directions (heart to breath [H2B] and breath to heart [B2H]).

As expected based on previous work, the transfer entropy from breath to heart was significantly higher than from heart to breath. Crucially, our analysis revealed that this effect is driven by two distinct Φ ID atoms, out of the four that comprise transfer entropy. The TE result is dominated by the $\text{Syn} \rightarrow \text{Un}$ atom, while the transfer atom itself ($\text{Un} \rightarrow \text{Un}$) shows no significant differences. Importantly, however, $\text{Un} \rightarrow \text{Red}$ shows a significant effect in the *opposite* direction to the main TE result. The standard TE analysis is unable to resolve these modes of information dynamics, and thus misses the heart’s unique contribution to the heart-breath joint dynamics.

In summary, Φ ID shows that the effect seen in the transfer entropy towards the heart is not transfer but synergistic, and that there is a smaller unique effect originating at the heart that is overshadowed by the former.¹⁰ These results illustrate the type of advantages that Φ ID can bring beyond standard transfer entropy and Granger causality analyses.

Discussion

This paper introduces Φ ID as a formal framework to study high-order interactions in the dynamics of multivariate complex systems. By bringing together aspects of integrated information theory (IIT) and partial information decomposition (PID), the Φ ID framework allows us to decompose multivariate information flow into interpretable, distinct parts. This decomposition brings two important outcomes. First, it allows us to better understand and refine existing metrics of information exchange and dynamical complexity. Second, it enables systematic analyses of previously unexplored modes of information dynamics, which are not captured by previous analysis methods.

Towards multi-dimensional accounts of dynamical complexity

Φ ID provides principled tools to inspect existing measures of information dynamics and overcome some of their shortcomings. In particular, we have shown that both the widely used transfer entropy and what is referred to as ‘integrated information’ in the context of IIT are in fact aggregates of several distinct information effects, typically including transfer and synergy phenomena. In addition, our analysis shows that different measures of integrated information actually capture different Φ ID atoms in various

¹⁰The study of the physiological implications of these findings will be investigated in a separate publication.

proportions, which provides a formal explanation for the heterogeneity among existing measures reported in Ref. [19].

Supporting our theoretical results, we showed in empirical physiological data that significant differences in transfer entropy can be observed even in the absence of genuine information transfer phenomena, highlighting the practical relevance of our framework. Likewise, our analysis based on whole-brain modelling showed how the conflation of fundamentally distinct information phenomena in existing measures of integrated information can introduce substantial confusion in the results and interpretation of neuroscientific analysis. Φ ID provides tools to identify these problems, and also to fix them, by tailoring measures that target the specific kinds of information dynamics one wishes to analyse.

As well as providing a new taxonomy of information dynamics phenomena, Φ ID establishes that there are fundamental limitations to any purported all-encompassing scalar measure of dynamical complexity, in line with Feldman and Crutchfield [57]. The space of possible complex dynamics is, unsurprisingly, vast and complex, and while scalar measures might still have great practical value in specific contexts,¹¹ Φ ID clarifies that a general theory of complex systems (biological or otherwise) cannot be reduced to a single, one-size-fits-all measure, but rather needs to embrace this richness.

Limitations and future extensions

Φ ID is a general tool to decompose multivariate mutual information, and the nature of the resulting decomposition critically depends on how the underlying joint distribution has been constructed. In particular, note that the Φ ID framework depends only on a joint probability distribution $p(\mathbf{X}_t, \mathbf{X}_{t+1})$, and thus its results can be interpreted as causality in the Pearl or Granger sense, depending on whether the distribution comes from intervention or observation, respectively. If the distribution is built on observational data then the decomposition generally should be understood in the Granger-causal sense (i.e. as referring to predictive ability). Similarly, if the conditional distribution $p(\mathbf{X}_{t+1}|\mathbf{X}_t)$ is equivalent to a $\text{do}()$ distribution in Pearl’s sense [5], and the system satisfies the faithfulness and causal Markov conditions, then the results of Φ ID are to be interpreted in a counterfactual causal sense. In either case, the formalism developed here applies directly.

Naturally, Φ ID inherits some characteristics of PID. In particular, Φ ID specifies the relationships between information atoms, but does not prescribe a particular functional form for them. To compute numerical values of Φ ID atoms one needs a double-redundancy function, a multi-target extension of PID’s redundancy function. In PID, several distinct redundancy functions have been proposed, and while they have been shown to agree in various scenarios [59], they may differ in other cases and there is not yet a consensus on one that is universally preferable [60]. The formulation of multiple double-redundancy functions, and a thorough comparison in simulated systems is an important line for future work.

Finally, it is important to remark that the framework presented in this paper focuses on decomposing the mutual information between two time points. While this captures all the information carried from past to future in Markovian systems, it might miss relevant phenomena in systems with non-Markovian dynamics – which typically arise in experimental data of scenarios with many non-observable variables. As an important extension, future work should investigate the effect of unobserved variables on the proposed decomposition, which could be done e.g. leveraging Taken’s embedding theorem [61, 62] or other methods [63].

¹¹For example, measures that accurately discriminate between neural configurations corresponding to conscious and unconscious states in a particular experimental paradigm [58].

Methods

This section establishes the mathematical bases of our framework. The aim is to build a decomposition of the TDMI, as defined in Eq. (1), that differentiates the role of each source and each target (possibly multivariate) variable – hence accounting for both cause (forward) and effect (backward) information simultaneously. To do this, our proposed decomposition brings together the partitions enabled by a forward PID (where variables at time t and $t + 1$ are sources and targets, respectively) and a backward PID (where the assignment of sources and targets is reversed), as illustrated in Figure 1a. By doing this, we overcome PID’s limitation of having only one single target variable and formulate a multi-target information decomposition.

Note that throughout this section we switch from the **Red/Un/Syn** notation above to the more standard (and more general) ‘curly bracket’ notation introduced by Williams and Beer [21].

Double-redundancy lattice

Let us start by reviewing the construction of the redundancy lattice that is employed in PID to formalise our intuitive understanding of redundancy [21]. This lattice is built over the set \mathcal{A} , which for the case of two time series can be expressed as

$$\mathcal{A} := \{\{1\}, \{2\}, \{1, 2\}, \{\{1\}, \{2\}\}\}, \quad (5)$$

which correspond to all the sets of subsets of $\{1, 2\}$ where no element is contained in another.¹² Then, the lattice is built using a natural (partial) order relationship that exists between the elements of \mathcal{A} [21]: for $\alpha, \beta \in \mathcal{A}$, one says that

$$\alpha \preceq \beta \quad \text{if} \quad \text{for all } b \in \beta \text{ there exists } a \in \alpha \text{ such that } a \subset b. \quad (6)$$

The lattice that encodes the relationship \preceq is known as the redundancy lattice (Fig. 1b), and guides the construction of the four terms in the PID.

Our first step in building the foundations of Φ ID is to build a *product lattice* over $\mathcal{A} \times \mathcal{A}$, in order to extend the notion of redundancy from PID to the case of multiple source and target variables (here X_t^1, X_t^2 and X_{t+1}^1, X_{t+1}^2 respectively). Intuitively, Φ ID is the ‘product’ of two complementary single-target PIDs, one decomposing the information carried by the past about the future, and the other decomposing the information carried by the future about the past (Fig. 1a). To formalise this intuition, we extend Williams and Beer’s [21] notation, and denote sets of sources and targets using their indices only with an arrow going from past to future. Hence, the nodes of the product lattice are denoted as $\alpha \rightarrow \beta$ for $\alpha, \beta \in \mathcal{A}$.

A natural partial ordering relationship can be established over the product lattice as follows:

$$\alpha \rightarrow \beta \preceq \alpha' \rightarrow \beta' \quad \text{iff} \quad \alpha \preceq \alpha' \text{ and } \beta \preceq \beta'. \quad (7)$$

This relationship establishes a lattice structure¹³, which for the case of a bipartite system consists of 16 nodes (Fig. 1c).

Redundancies and atoms

The other ingredient in the PID recipe – besides the redundancy lattice – is a *redundancy function*, I_\cap , that quantifies the amount of ‘overlapping’ information about

¹²For a case of N variables, then \mathcal{A} is the set of antichains on the lattice $(\mathcal{P}(\{1, \dots, N\}), \subseteq)$, discussed in Ref. [21]. We focus on the bivariate case for clarity, although the Φ ID formalism developed here can be applied to any N .

¹³A proof of this is provided in the Appendix.

the target that is common to a set of sources $\alpha \in \mathcal{A}$ [21]. The redundancy function in a PID, I_{\cap}^{α} , encompasses the following terms in the case of two source variables:

- $I_{\cap}^{\{1\}\{2\}}$ is the information about the target that is in either source,
- $I_{\cap}^{\{i\}}$ is the information in source i , and
- $I_{\cap}^{\{12\}}$ is the information that is in both sources when considered together.

This subsection extends the notion of overlapping information to the multi-target setting.

For a given $\alpha \rightarrow \beta \in \mathcal{A} \times \mathcal{A}$, the overlapping information that is common to sources α and can be seen in targets β is denoted as $I_{\cap}^{\alpha \rightarrow \beta}$ and referred to as the *double-redundancy function*. In the following, we assume that the double-redundancy function satisfies two axioms:

- **Axiom 1 (compatibility)**: if $\alpha = \{\alpha_1, \dots, \alpha_J\}$ and $\beta = \{\beta_1, \dots, \beta_K\}$ with $\alpha, \beta \in \mathcal{A}$ and α_j, β_k non-empty subsets of $\{1, \dots, N\}$, then the following cases can be reduced to the redundancy of PID or the mutual information:¹⁴

$$I_{\cap}^{\alpha \rightarrow \beta} = \begin{cases} \text{Red}(\mathbf{X}_t^{\alpha_1}, \dots, \mathbf{X}_t^{\alpha_J}; \mathbf{X}_{t'}^{\beta_1}) & \text{if } K = 1, \\ \text{Red}(\mathbf{X}_{t'}^{\beta_1}, \dots, \mathbf{X}_{t'}^{\beta_K}; \mathbf{X}_t^{\alpha_1}) & \text{if } J = 1, \\ I(\mathbf{X}_t^{\alpha_1}, \mathbf{X}_{t'}^{\beta_1}) & \text{if } J = K = 1. \end{cases}$$

- **Axiom 2 (partial ordering)**: if $\alpha \rightarrow \beta \preceq \alpha' \rightarrow \beta'$ then $I_{\cap}^{\alpha \rightarrow \beta} \leq I_{\cap}^{\alpha' \rightarrow \beta'}$.

Intuitively, the first axiom guarantees that any double-redundancy function in ΦID reduces to a PID-type redundancy function when evaluated in certain atoms, and the second encapsulates the basic desideratum of the double-redundancy being in agreement with the partial ordering given by the product lattice.

By exploiting these two axioms, one can define ‘atoms’ that belong to each of the nodes via the Moebius inversion formula. Concretely, the ΦID atoms $I_{\partial}^{\alpha \rightarrow \beta}$ are defined as the quantities that guarantee the following condition for all $\alpha \rightarrow \beta \in \mathcal{A} \times \mathcal{A}$:

$$I_{\cap}^{\alpha \rightarrow \beta} = \sum_{\alpha' \rightarrow \beta' \preceq \alpha \rightarrow \beta} I_{\partial}^{\alpha' \rightarrow \beta'}. \quad (8)$$

In other words, $I_{\partial}^{\alpha \rightarrow \beta}$ corresponds to the information contained in node $\alpha \rightarrow \beta$ and not in any node below it in the lattice. These are analogues to the redundant, unique, and synergistic atoms in standard PID, but using the product lattice as a scaffold. By inverting this relationship, one can find a recursive expression for calculating I_{∂} as

$$I_{\partial}^{\alpha \rightarrow \beta} = I_{\cap}^{\alpha \rightarrow \beta} - \sum_{\alpha' \rightarrow \beta' \prec \alpha \rightarrow \beta} I_{\partial}^{\alpha' \rightarrow \beta'}. \quad (9)$$

With all the tools at hand, we can deliver the promised decomposition of the TDMI in terms of atoms of integrated information, as established in the next definition.

Definition 1. *The Integrated Information Decomposition (ΦID) of a system with Markovian dynamics is the collection of atoms I_{∂} defined from the redundancies I_{\cap} via Eq. (9), which satisfy*

$$\text{TDMI} = I(\mathbf{X}_t; \mathbf{X}_{t'}) = \sum_{\alpha, \beta \in \mathcal{A}} I_{\partial}^{\alpha \rightarrow \beta}. \quad (10)$$

¹⁴Here we use the shorthand notation $\mathbf{X}_t^{\alpha} := (X_t^{i_1}, \dots, X_t^{i_K})$ for $\alpha = \{i_1, \dots, i_K\}$.

In this way, the Φ ID of two time series gives 16 atoms that correspond to the lattice shown in Figure 1c, which are computed via a linear transformation over the 16 redundancies. Importantly, Axioms 1 and 2 allow us to compute all the I_{\cap} terms once a single-target PID redundancy function $\text{Red}(\cdot)$ has been chosen with the sole exception of $I_{\cap}^{\{1\}\{2\} \rightarrow \{1\}\{2\}}$.¹⁵ All this is summarised in the following result.

Proposition 1 (15-for-free). *Axioms 1 and 2 provide unique values for the 16 atoms of the product lattice after one defines (i) a single-target redundancy function $\text{Red}(\cdot)$, and (ii) an expression for $I_{\delta}^{\{1\}\{2\} \rightarrow \{1\}\{2\}}$.*

Therefore, in the same way as in PID the definition of $\text{Red}(\cdot)$ gives 3 other terms (unique and synergy) as side-product, Proposition 1 shows that in Φ ID the addition of the double-redundancy function $I_{\delta}^{\{1\}\{2\} \rightarrow \{1\}\{2\}}$ gives the 15 other terms for free. In the Supplementary Material we describe Φ ID extensions of two common PID redundancy functions (Ince’s CCS [39] and Barrett’s MMI [40] measures), which we use for all numerical examples in this paper.

Supporting information

S1 Appendix. Proofs and technical details.

Acknowledgments

The authors thank Julian Sutherland for valuable discussions. P.A.M.M. was supported by the Wellcome Trust (grant number 210920/Z/18/Z). F.E.R. was supported by the Ad Astra Chandaria Foundation, and by the European Union’s H2020 research and innovation programme under the Marie Skłodowska-Curie grant agreement No. 702981. A.I.L. is supported by a Gates Cambridge Scholarship. A.K.S. and A.B.B. acknowledge support from the Dr Mortimer and Theresa Sackler Foundation. A.K.S. also acknowledges support from the Canadian Institute for Advanced Research (CIFAR) Program on Brain, Mind, and Consciousness.

References

1. Kelso JS. Dynamic Patterns: The Self-organization of Brain and Behavior. MIT Press; 1995.
2. Runge J, Bathiany S, Bollt E, Camps-Valls G, Coumou D, Deyle E, et al. Inferring causation from time series in Earth system sciences. Nature Communications. 2019;10(1):2553.
3. Dosi G, Roventini A. More is different ... and complex! The case for agent-based macroeconomics. J Evol Econ. 2019;29(1).
4. Bressler SL, Seth AK. Wiener–Granger causality: A well established methodology. NeuroImage. 2011;58(2):323–329.
5. Pearl J, Mackenzie D. The Book of Why: The New Science of Cause and Effect. Basic Books; 2018.

¹⁵This can be verified directly by studying the coefficients of the linear system of equations that relate redundancies and atoms.

6. Chan TE, Stumpf MP, Babbie AC. Gene regulatory network inference from single-cell data using multivariate information measures. *Cell systems*. 2017;5(3):251–267.
7. Scagliarini T, Faes L, Marinazzo D, Stramaglia S, Mantegna RN. Synergistic information transfer in the global system of financial markets. *Entropy*. 2020;22(9):1000.
8. Rosas FE, Mediano PA, Gastpar M, Jensen HJ. Quantifying high-order interdependencies via multivariate extensions of the mutual information. *Physical Review E*. 2019;100(3):032305. doi:10.1103/PhysRevE.100.032305.
9. Wibral M, Phillips WA, Lizier JT, Priesemann V. Partial information decomposition as a unified approach to the characterization and design of neural goal functions. *BMC neuroscience*. 2015;16(1):1–2.
10. Luppi AI, Mediano PA, Rosas FE, Holland N, Fryer TD, O’Brien JT, et al. A synergistic core for human brain evolution and cognition. *bioRxiv*. 2020;.
11. Luppi AI, Mediano PA, Rosas FE, Allanson J, Pickard JD, Carhart-Harris RL, et al. A Synergistic Workspace for Human Consciousness Revealed by Integrated Information Decomposition. *bioRxiv*. 2020;.
12. Grassberger P. Toward a quantitative theory of self-generated complexity. *International Journal of Theoretical Physics*. 1986;25(9):907–938.
13. Crutchfield JP, Feldman DP. Regularities unseen, randomness observed: Levels of entropy convergence. *Chaos: An Interdisciplinary Journal of Nonlinear Science*. 2003;13(1):25–54.
14. Tononi G, Sporns O, Edelman G. A measure for brain complexity: Relating functional segregation and integration in the nervous system. *Proceedings of the National Academy of Sciences*. 1994;91(11):5033–5037.
15. Balduzzi D, Tononi G. Integrated information in discrete dynamical systems: Motivation and theoretical framework. *PLoS Computational Biology*. 2008;4(6):1–18.
16. Oizumi M, Albantakis L, Tononi G. From the phenomenology to the mechanisms of consciousness: Integrated information theory 3.0. *PLoS Computational Biology*. 2014;10(5).
17. Seth AK, Barrett AB, Barnett L. Causal density and integrated information as measures of conscious level. *Philosophical Transactions of the Royal Society A: Mathematical, Physical and Engineering Sciences*. 2011;369(1952):3748–3767.
18. van Walsum AMvC, Pijnenburg Y, Berendse H, van Dijk B, Knol D, Scheltens P, et al. A neural complexity measure applied to MEG data in Alzheimer’s disease. *Clinical Neurophysiology*. 2003;114(6):1034–1040.
19. Mediano P, Seth A, Barrett A. Measuring integrated information: Comparison of candidate measures in theory and simulation. *Entropy*. 2019;21(1):17.
20. James RG, Barnett N, Crutchfield JP. Information flows? A critique of transfer entropies. *Physical Review Letters*. 2016;116(23):238701.
21. Williams PL, Beer RD. Nonnegative decomposition of multivariate information; 2010.

22. Finn C, Lizier JT. Quantifying information modification in cellular automata using pointwise partial information decomposition. In: *Artificial Life Conference Proceedings*. MIT Press; 2018. p. 386–387.
23. Rosas F, Mediano P, Ugarte M, Jensen H. An information-theoretic approach to self-organisation: Emergence of complex interdependencies in coupled dynamical systems. *Entropy*. 2018;20(10):793.
24. Beer RD, Williams PL. Information processing and dynamics in minimally cognitive agents. *Cognitive Science*. 2015;39(1):1–38. doi:10.1111/cogs.12142.
25. Tax TMS, Mediano PAM, Shanahan M. The Partial Information Decomposition of Generative Neural Network Models. *Entropy*. 2017;19(9). doi:10.3390/e19090474.
26. Varley TF. Intersectional synergies: Untangling irreducible effects of intersecting identities via information decomposition. *arXiv:210610338*. 2021;.
27. Cang Z, Nie Q. Inferring spatial and signaling relationships between cells from single cell transcriptomic data. *Nature Communications*. 2020;11(1):1–13. doi:10.1038/s41467-020-15968-5.
28. Seth AK. Measuring autonomy and emergence via Granger causality. *Artificial Life*. 2010;16(2):179–196.
29. Rosas FE, Mediano PA, Jensen HJ, Seth AK, Barrett AB, Carhart-Harris RL, et al.. Reconciling emergences: An information-theoretic approach to identify causal emergence in multivariate data; 2020.
30. Lizier J. *The Local Information Dynamics of Distributed Computation in Complex Systems*. University of Sydney; 2010.
31. Mediano PAM, Farah JC, Shanahan M. Integrated Information and Metastability in Systems of Coupled Oscillators. *ArXiv e-prints*. 2016;.
32. Aguilera M, Di Paolo E. Integrated information in the thermodynamic limit. *Neural Networks*. 2019;.
33. Mediano PA, Rosas FE, Farah JC, Shanahan M, Bor D, Barrett AB. Integrated information as a common signature of dynamical and information-processing complexity. *arXiv preprint arXiv:210610211*. 2021;.
34. Barrett AB, Seth AK. Practical measures of integrated information for time-series data. *PLoS Computational Biology*. 2011;7(1):1–18.
35. Tegmark M. Improved measures of integrated information. *PLoS Computational Biology*. 2016;12(11):e1005123. doi:10.1371/journal.pcbi.1005123.
36. Griffith V. A principled infotheoretic φ -like measure; 2014.
37. Oizumi M, Tsuchiya N, Amari Si. Unified framework for information integration based on information geometry. *Proceedings of the National Academy of Sciences*. 2016;113(51):14817–14822.
38. Deco G, Vidaurre D, Kringelbach ML. Revisiting the global workspace orchestrating the hierarchical organization of the human brain. *Nature Human Behaviour*. 2021;5(4):497–511. doi:10.1038/s41562-020-01003-6.

39. Ince RAA. Measuring Multivariate Redundant Information with Pointwise Common Change in Surprisal. *Entropy*. 2017;19(7). doi:10.3390/e19070318.
40. Barrett AB. Exploration of synergistic and redundant information sharing in static and dynamical Gaussian systems. *Phys Rev E*. 2015;91:052802.
41. Finn C, Lizier JT. Pointwise partial information decomposition using the specificity and ambiguity lattices. *Entropy*. 2018;20(4):297. doi:10.3390/e20040297.
42. McGill WJ. Multivariate information transmission. *Psychometrika*. 1954;19(2):97–116.
43. Deco G, Ponce-Alvarez A, Hagmann P, Romani GL, Mantini D, Corbetta M. How local excitation-inhibition ratio impacts the whole brain dynamics. *Journal of Neuroscience*. 2014;34(23):7886–7898.
44. Deco G, Jirsa VK. Ongoing cortical activity at rest: Criticality, multistability, and ghost attractors. *Journal of Neuroscience*. 2012;32(10):3366–3375. doi:10.1523/JNEUROSCI.2523-11.2012.
45. Deco G, Ponce-Alvarez A, Mantini D, Romani GL, Hagmann P, Corbetta M. Resting-state functional connectivity emerges from structurally and dynamically shaped slow linear fluctuations. *Journal of Neuroscience*. 2013;33(27):11239–11252. doi:10.1523/JNEUROSCI.1091-13.2013.
46. Hansen EC, Battaglia D, Spiegler A, Deco G, Jirsa VK. Functional connectivity dynamics: Modeling the switching behavior of the resting state. *NeuroImage*. 2015;105:525–535. doi:10.1016/j.neuroimage.2014.11.001.
47. Friston KJ, Mechelli A, Turner R, Price CJ. Nonlinear responses in fMRI: The Balloon model, Volterra kernels, and other hemodynamics. *NeuroImage*. 2000;12(4):466–477. doi:10.1006/ning.2000.0630.
48. Ipiña IP, Kehoe PD, Kringelbach M, Laufs H, Ibañez A, Deco G, et al. Modeling regional changes in dynamic stability during sleep and wakefulness. *NeuroImage*. 2020;215:116833. doi:10.1016/j.neuroimage.2020.116833.
49. Luppi AI, Mediano PA, Rosas FE, Allanson J, Pickard JD, Williams GB, et al. Paths to oblivion: Common neural mechanisms of anaesthesia and disorders of consciousness. *bioRxiv*. 2021;doi:10.1101/2021.02.14.431140.
50. Herzog R, Mediano PAM, Rosas FE, Carhart-Harris R, Sanz Y, Tagliazucchi E, et al. A mechanistic model of the neural entropy increase elicited by psychedelic drugs. *Scientific Reports*. 2020;10(17725).
51. Glasser MF, Sotiropoulos SN, Wilson JA, Coalson TS, Fischl B, Andersson JL, et al. The minimal preprocessing pipelines for the Human Connectome Project. *NeuroImage*. 2013;80:105–124.
52. Deco G, Cruzat J, Cabral J, Knudsen GM, Carhart-Harris RL, Whybrow PC, et al. Whole-brain multimodal neuroimaging model using serotonin receptor maps explains non-linear functional effects of LSD. *Current Biology*. 2018; p. 1–10.
53. Nemati S, Edwards BA, Lee J, Pittman-Polletta B, Butler JP, Malhotra A. Respiration and heart rate complexity: effects of age and gender assessed by band-limited transfer entropy. *Respiratory Physiology & Neurobiology*. 2013;189(1):27–33.

54. Pini N, Lucchini M, Fifer WP, Burtchen N, Signorini MG, et al. Lagged transfer entropy analysis to investigate cardiorespiratory regulation in newborns during sleep. In: *BIOSTEC-BIOSIGNALS*. SCITEPRESS; 2019. p. 139–146.
55. de Abreu RM, Catai AM, Cairo B, Rehder-Santos P, da Silva CD, Signini ÉDF, et al. A transfer entropy approach for the assessment of the impact of inspiratory muscle training on the cardiorespiratory coupling of amateur cyclists. *Frontiers in Physiology*. 2020;11.
56. Iyengar N, Peng C, Morin R, Goldberger AL, Lipsitz LA. Age-related alterations in the fractal scaling of cardiac interbeat interval dynamics. *American Journal of Physiology – Regulatory, Integrative and Comparative Physiology*. 1996;271(4):R1078–R1084.
57. Feldman DP, Crutchfield JP. Measures of statistical complexity: Why? *Physics Letters A*. 1998;238(4-5):244–252.
58. Casali AG, Gosseries O, Rosanova M, Boly M, Sarasso S, Casali KR, et al. A theoretically based index of consciousness independent of sensory processing and behavior. *Science Translational Medicine*. 2013;5(198):198ra105.
59. Rosas FE, Mediano PA, Rassouli B, Barrett AB. An operational information decomposition via synergistic disclosure. *Journal of Physics A: Mathematical and Theoretical*. 2020;53(48):485001. doi:10.1088/1751-8121/abb723.
60. James RG, Emenheiser J, Crutchfield JP. Unique information via dependency constraints. *Journal of Physics A: Mathematical and Theoretical*. 2018;52(1):014002.
61. Takens F. Detecting strange attractors in turbulence. In: *Dynamical Systems and Turbulence*. Springer; 1981. p. 366–381.
62. Cliff OM, Prokopenko M, Fitch R. An information criterion for inferring coupling of distributed dynamical systems. *Frontiers in Robotics and AI*. 2016;3:71.
63. Wilting J, Priesemann V. Inferring collective dynamical states from widely unobserved systems. *Nature Communications*. 2018;9(1):1–7.

Supporting Information for

Towards an extended taxonomy of information dynamics via
Integrated Information Decomposition

Pedro A.M. Mediano,^{1,*} Fernando E. Rosas,^{2,3,4,*} Andrea I. Luppi,^{5,6,7}
Robin L. Carhart-Harris,² Daniel Bor,¹ Anil K. Seth,⁸ and Adam B. Barrett^{8,9}

¹*Department of Psychology, University of Cambridge, Cambridge, UK*

²*Centre for Psychedelic Research, Imperial College London, London, UK*

³*Data Science Institute, Imperial College London, London, UK*

⁴*Center for Complexity Science, Imperial College London, London, UK*

⁵*University Division of Anaesthesia, University of Cambridge, Cambridge, UK*

⁶*Department of Clinical Neurosciences, University of Cambridge, Cambridge, UK*

⁷*Leverhulme Centre for the Future of Intelligence, University of Cambridge, Cambridge, UK*

⁸*Sackler Center for Consciousness Science, University of Sussex, Brighton, UK*

⁹*The Data Intensive Science Centre, University of Sussex, Brighton, UK*

(Dated: September 28, 2021)

I. THE PRODUCT OF TWO LATTICES IS A LATTICE

A lattice is a partially ordered set (\mathcal{A}, \preceq) for which every pair of elements a, b has a well-defined *meet* $a \wedge b$ and *join* $a \vee b$, which correspond to their common greatest lower bound (infimum) and common least upper bound (supremum), respectively [1]. Here we prove that, if (\mathcal{A}, \preceq) is a lattice, then the product lattice $(\mathcal{A} \times \mathcal{A}, \preceq^*)$ equipped with the order relationship

$$\alpha \rightarrow \beta \preceq^* \alpha' \rightarrow \beta' \quad \text{if and only if} \quad \alpha \preceq \alpha' \quad \text{and} \quad \beta \preceq \beta', \quad (1)$$

is also a lattice, where $\alpha, \beta, \alpha', \beta' \in \mathcal{A}$. As a corollary of this, given that the set and partial ordering relationship used in PID are a lattice [2, 3], then the set and partial ordering relationship used in Φ ID are also a lattice.

For compactness, let us use the notation $\gamma = \alpha \rightarrow \beta$ and $\gamma' = \alpha' \rightarrow \beta'$ for $\gamma, \gamma' \in \mathcal{A} \times \mathcal{A}$. To prove the lattice structure of $(\mathcal{A} \times \mathcal{A}, \preceq^*)$ it suffices to show that

1. $\gamma \wedge^* \gamma' := \alpha \wedge \alpha' \rightarrow \beta \wedge \beta'$ is a valid meet; and
2. $\gamma \vee^* \gamma' := \alpha \vee \alpha' \rightarrow \beta \vee \beta'$ is a valid join.

Note that the fact that (\mathcal{A}, \preceq) is a lattice implies that $\alpha \wedge \beta$ and $\alpha \vee \beta$ are well-defined for all $\alpha, \beta \in \mathcal{A}$.

Let us begin with the meet, for which we use $m = \gamma \wedge^* \gamma'$ as a shorthand notation. First, one can directly check that $m \preceq^* \gamma$ and $m \preceq^* \gamma'$, given the definition of \preceq^* above and the fact that $\alpha \wedge \alpha' \preceq \alpha$ (and similarly for α', β , and β'). Next, we need to prove that for any $\gamma'' = \alpha'' \rightarrow \beta'' \in \mathcal{A} \times \mathcal{A}$ such that $\gamma'' \preceq^* \gamma$ and $\gamma'' \preceq^* \gamma'$, we have $\gamma'' \preceq^* m$ (i.e. that m is the greatest lower bound of γ and γ'). To see this, note that the conditions $\gamma'' \preceq^* \gamma$ and $\gamma'' \preceq^* \gamma'$ imply the following four statements:

$$\begin{aligned} \alpha'' &\preceq \alpha, \\ \alpha'' &\preceq \alpha', \\ \beta'' &\preceq \beta, \\ \beta'' &\preceq \beta'. \end{aligned}$$

Using these relationships and the \wedge operator from \mathcal{A} , one can show that $\alpha'' \preceq \alpha \wedge \alpha'$ and $\beta'' \preceq \beta \wedge \beta'$, which in turn implies that $\gamma'' \preceq^* m$. Finally, the proof for the join is analogous, replacing \wedge with \vee and \preceq with \succeq .

* P.M. and F.R. contributed equally to this work.
E-mail: pam83@cam.ac.uk; f.rosas@imperial.ac.uk

II. DECOMPOSING PID ATOMS

Equation (4) in the main text shows how to decompose redundancies in the product lattice in terms of Φ ID atoms. Here we provide a more general statement, that allows us to decompose not only redundancies, but also other PID atoms. The goal of this appendix is to build stronger connections between PID and Φ ID, and to extend Proposition 1 to allow greater flexibility for specifying a Φ ID function.

Note that the Φ ID framework applies to any pair of sets of source and target variables, which need not correspond to the past and future states of a dynamical system. To highlight the generality of the Φ ID framework, for the rest of this supplementary material we use the notation $\mathbf{X} = \{X_1, X_2, \dots\}$ to refer to the sources, and analogously $\mathbf{Y} = \{Y_1, Y_2, \dots\}$ for the targets. The expressions in the main text can be recovered by simply setting $\mathbf{X} := \mathbf{X}_t, \mathbf{Y} := \mathbf{X}_{t+1}$.

For the forward PID, and borrowing the notation from Williams and Beer [2], given a non-empty set of ‘future’ variables $F \in \mathcal{P}(\{Y_1, \dots, Y_N\})$ and an element of the redundancy lattice $\alpha \in \mathcal{A}$, let us denote by $\Pi_F(\alpha; F)$ the α atom of the PID decomposition for $I(\mathbf{X}; F)$, such that

$$I(\mathbf{X}; F) = \sum_{\alpha \in \mathcal{A}} \Pi_F(\alpha; F) . \quad (2)$$

We use an analogous notation for the backward PID, with a corresponding non-empty set of ‘past’ variables $P \in \mathcal{P}(\{X_1, \dots, X_N\})$ and $\beta \in \mathcal{A}$, such that

$$I(P; \mathbf{Y}) = \sum_{\beta \in \mathcal{A}} \Pi_B(P; \beta) . \quad (3)$$

Then, these quantities can be further decomposed in Φ ID atoms as

$$\Pi_F(\alpha; F) = \sum_{\gamma \preceq F} I_{\theta}^{\alpha \rightarrow \gamma} , \quad (4a)$$

$$\Pi_B(P; \beta) = \sum_{\gamma \preceq P} I_{\theta}^{\gamma \rightarrow \beta} . \quad (4b)$$

Note that the sum runs only across one of the sets (instead of both as it does in Eq. (4) of the main text), and that every element in $\mathcal{P}(\{1, \dots, N\})$ is also in \mathcal{A} , and hence the partial order relationship in the sums above is well-defined. As a few examples, in a bivariate system the following forward PID atoms decompose as:

$$\begin{aligned} \text{Red}(X_1, X_2; Y_i) &= \Pi_F(\{1\}\{2\}; Y_i) \\ &= I_{\theta}^{\{1\}\{2\} \rightarrow \{1\}\{2\}} + I_{\theta}^{\{1\}\{2\} \rightarrow \{i\}} , \end{aligned}$$

$$\begin{aligned} \text{Syn}(X_1, X_2; Y_i) &= \Pi_F(\{12\}; Y_i) \\ &= I_{\theta}^{\{12\} \rightarrow \{1\}\{2\}} + I_{\theta}^{\{12\} \rightarrow \{i\}} , \end{aligned}$$

$$\begin{aligned} \text{Un}(X_1; Y_1 Y_2 | X_2) &= \Pi_F(\{1\}; Y_1 Y_2) \\ &= I_{\theta}^{\{1\} \rightarrow \{1\}\{2\}} + I_{\theta}^{\{1\} \rightarrow \{1\}} \\ &\quad + I_{\theta}^{\{1\} \rightarrow \{2\}} + I_{\theta}^{\{1\} \rightarrow \{12\}} . \end{aligned}$$

These decompositions can be used to prove Proposition 1 of the main text. Adopting a view of Φ ID as a linear system of equations, one needs 16 independent equations to solve for the 16 unknowns that are the Φ ID atoms. Of those, 9 are given by standard Shannon mutual information (specifically, $I(X_i; Y_j)$, $I(X_1 X_2; Y_i)$, $I(Y_1 Y_2; X_i)$, and $I(X_1 X_2; Y_1 Y_2)$, for $i, j = \{1, 2\}$) decomposed with Eq. (4) of the main text, and 6 are given by the single-target PIDs ($\text{Red}(X_1, X_2; Y_1)$, $\text{Red}(X_1, X_2; Y_2)$, and $\text{Red}(X_1, X_2; Y_1 Y_2)$, as well as the 3 corresponding backward PIDs) decomposed by the expression above. Finally, one only need to add one individual Φ ID atom to make the 16 equations needed, and the system can be solved for all other atoms.

Taking these results together, Proposition 1 in the main text can be generalised as follows: a valid Φ ID can be defined not only in terms of redundancy, but also in terms of unique information or synergy. This is equivalent to the case of PID, for which decompositions based on unique information [4] or synergy [5, 6] have been proposed.

III. COMPUTING THE Φ ID ATOMS

Computation of Φ ID proceeds following the same general steps as in PID: first the intersection information $I_{\cap}^{\alpha \rightarrow \beta}$ is computed for every node; and then the integrated information atoms $I_{\partial}^{\alpha \rightarrow \beta}$ are obtained as the solution to a linear system of equations representing the Moebius inversion.

To compute the double-redundancy atom, $I_{\partial}^{\{1\}\{2\} \rightarrow \{1\}\{2\}}$, for numerical applications, we assume all systems are distributed as a multivariate Gaussian distribution, and use a Φ ID extension of Ince's *Common Change in Surprisal* (CCS) redundancy function [7]. As per the compatibility axiom, we formulate a multi-target CCS function that reduces to the original when only a single target is specified.

In line with Ince [7], we define $I_{\partial, \text{CCS}}^{\{1\}\{2\} \rightarrow \{1\}\{2\}}$ using pointwise (or *local*) information measures [8]. As a first step, we use the inclusion-exclusion principle to formulate a local 'multi-target co-information' $c(\mathbf{x}; \mathbf{y})$, defined as

$$c(\mathbf{x}; \mathbf{y}) := \sum_{\alpha \rightarrow \beta \in \overline{\mathcal{A}^2}} (-1)^{f(\alpha, \beta) + 1} i_{\cap}^{\alpha \rightarrow \beta}(\mathbf{x}; \mathbf{y}), \quad (5)$$

where $i_{\cap}^{\alpha \rightarrow \beta}(\mathbf{x}; \mathbf{y})$ is the pointwise redundancy function, $\overline{\mathcal{A}^2}$ is the set of nodes in the product lattice excluding the lowest node, and $f(\alpha, \beta) = \sum_{a \in \alpha} |a| + \sum_{b \in \beta} |b|$ [9]. Note that $i_{\cap}^{\alpha \rightarrow \beta}(\mathbf{x}; \mathbf{y})$ above corresponds to the standard pointwise mutual information and a single-target PID redundancy function, which we take here to be the usual CCS function as defined by Ince [7]. For the bivariate Φ ID, a formal calculation shows that

$$c(\mathbf{x}; \mathbf{y}) = i_{\partial}^{\{1\}\{2\} \rightarrow \{1\}\{2\}}(\mathbf{x}; \mathbf{y}) - i_{\partial}^{\{12\} \rightarrow \{12\}}(\mathbf{x}; \mathbf{y}).$$

Please note that, as for the co-information in the standard PID case, $c(\mathbf{x}; \mathbf{y})$ is a 'whole-minus-sum' measure [10] that can be computed without any Φ ID atoms explicitly. Then, as the second step in the definition, given a large set of M samples $\{\mathbf{x}^{(i)}, \mathbf{y}^{(i)}\}_{i=1}^M$ we define the set $\mathcal{S} \subseteq \{1, \dots, M\}$ as the subset of samples for which all marginal pointwise mutual informations, as well as the pointwise full mutual information $i(\mathbf{x}; \mathbf{y})$, have the same sign. With this, we are finally able to define the Gaussian CCS double-redundancy function.

Definition 1. Double-redundancy based on common change in surprisal. For a given set of variables (\mathbf{X}, \mathbf{Y}) , the double-redundancy based on common change in surprisal is defined as

$$I_{\partial, \text{CCS}}^{\{1\}\{2\} \rightarrow \{1\}\{2\}} := \sum_{i \in \mathcal{S}} c(\mathbf{x}^{(i)}; \mathbf{y}^{(i)}) \quad (6)$$

To show the presented results do not depend on the specific choice of the CCS function, we also formulate a Φ ID extension of the *Minimum Mutual Information* (MMI) PID [11]:

Definition 2. Double-redundancy based on minimum mutual information. For a given set of variables (\mathbf{X}, \mathbf{Y}) , the double-redundancy based on minimum mutual information is defined as

$$I_{\partial, \text{MMI}}^{\{1\}\{2\} \rightarrow \{1\}\{2\}} := \min_{i, j} I(X_i; Y_j). \quad (7)$$

In both cases (CCS and MMI), it is direct to check the proposed definitions satisfy the compatibility axiom with respect to their original PID definitions [7, 11]. At the same time, and although the extensions presented here seem the most natural, they are not the only possible ones that are compatible with the originals, and in principle any function that satisfies the double-redundancy axioms can be used to compute Φ ID.

IV. RESULTS OF SECTION 'DIFFERENT TYPES OF INTEGRATION'

Here we present calculations for the example systems in Fig. 4 of the main text. These proofs hold for all Φ ID that satisfy the partial ordering axiom of $I_{\cap}^{\alpha \rightarrow \beta}$ (Axiom 2 in the main text), have a non-negative double-redundancy function $I^{\{1\}\{2\} \rightarrow \{1\}\{2\}} \geq 0$, and satisfy the following bound that follows from the basic properties of PID (c.f. [12]):

$$\text{Red}(X, Y; Z) \leq \min\{I(X; Z), I(Y; Z)\}. \quad (8)$$

Let us examine the three systems in turn:

- For the copy transfer system, $Y_2 = X_1$, while X_2 and Y_2 are independent i.i.d. fair coin flips. Since Y_2 is independent from the rest of the system, $\text{Red}(X_1, X_2; Y_2) = \text{Red}(X_1, X_2; Y_2) = 0$, and due to partial ordering $I_{\cap}^{\{1\}\{2\} \rightarrow \{1\}\{2\}} = 0$. Finally, using the Moebius inversion formula it follows that $I_{\partial}^{\{1\} \rightarrow \{2\}} = I(X_1; Y_2) = 1$ and all other atoms are zero.
- In the downward XOR system, X_1 and X_2 are i.i.d. fair coin flips, $Y_1 = X_1 \oplus X_2$, and Y_2 is independent of the rest. Then, it is clear that $I(X_1, X_2; Y_1, Y_2) = I(X_1, X_2; Y_1) = 1$, while $I(X_1; Y_1) = I(X_2; Y_1) = 0$. Additionally, note that $I_{\cap}^{\{12\} \rightarrow \{1\}\{2\}} = 0$, since $\text{Red}(Y_1, Y_2; X_1 X_2) \leq I(Y_2; X_1 X_2) = 0$. All this implies that all the redundancies (and hence all the atoms) below $\{12\} \rightarrow \{1\}$ are zero, and hence $I_{\partial}^{\{12\} \rightarrow \{1\}} = 1$ due to the Moebius inversion formula.
- Finally, consider the PPR system where X_1, X_2, Y_1 are i.i.d. fair coin flips and Y_2 is such that $X_1 \oplus X_2 = Y_1 \oplus Y_2$. Then $I(X_1, X_2; Y_1) = I(X_1, X_2; Y_2) = I(X_1; Y_1, Y_2) = I(X_2; Y_1, Y_2) = 0$. This implies that all redundancies (and hence atoms) except $I_{\cap}^{\{12\} \rightarrow \{12\}}$ are zero, and hence using again the Moebius inversion formula $I_{\partial}^{\{12\} \rightarrow \{12\}} = I(X_1, X_2; Y_1, Y_2) = 1$.

V. RESULTS RELATED TO MEASURES OF INTEGRATED INFORMATION

In this appendix we prove the results in Table 1 of the main text, that shows whether each of four measures of integrated information (Φ^{WMS} , CD, ψ , Φ_G) are positive, negative, or zero in a system containing only one ΦID atom. A succinct definition of each measure is given below, and a comprehensive review and comparison of these and other measures can be found in Ref. [13].

Throughout this section we focus on bivariate systems, and use i, j as variable indices, with $i \neq j$. To complete the proof we will first show that it is possible to build systems with exactly one bit of information in one ΦID atom, and we will then compute the four measures on those systems.

Let us begin with the design of systems with one specific ΦID atom. Intuitively, this can be accomplished with a suitable combination of COPY and XOR gates for redundant and synergistic sets of variables, respectively. More formally, the procedure to build a system with $I_{\partial}^{\alpha \rightarrow \beta} = 1$ and all other atoms equal to zero is as follows:

1. Sample w from a Bernoulli distribution with $p = 0.5$.
2. Sample \mathbf{x} based on α :
 - If $\alpha = \{1\}\{2\}$, then $x_1 = x_2 = w$.
 - If $\alpha = \{i\}$, then $x_i = w$ and x_j is sampled from a Bernoulli distribution with $p = 0.5$.
 - If $\alpha = \{12\}$, then \mathbf{x} is a random string with parity w .
3. Sample \mathbf{y} based on β analogously.

In all cases there will be one bit of information (w) shared between \mathbf{X} and \mathbf{Y} , hence $I(\mathbf{X}; \mathbf{Y}) = 1$ for any choice of α, β . This can be proven using the fact that for any α, β , one has $H(W) = 1$, $H(W|\mathbf{X}) = H(W|\mathbf{Y}) = 0$, and $p(\mathbf{x}, \mathbf{y}, w) = p(\mathbf{x}|w)p(\mathbf{y}|w)p(w)$. To do so, let us start from the mutual information chain rule:

$$\begin{aligned} I(\mathbf{X}; \mathbf{Y}W) &= I(\mathbf{X}; W) + I(\mathbf{X}; \mathbf{Y}|W) \\ &= I(\mathbf{X}; \mathbf{Y}) + I(\mathbf{X}; W|\mathbf{Y}) . \end{aligned}$$

Rearranging the above terms, one can find that

$$I(\mathbf{X}; \mathbf{Y}) = I(\mathbf{X}; W) + I(\mathbf{X}; \mathbf{Y}|W) - I(\mathbf{X}; W|\mathbf{Y}) ,$$

where $I(\mathbf{X}; W) = H(W) - H(W|\mathbf{X}) = 1$ and $I(\mathbf{X}; \mathbf{Y}|W) = 0$. Finally, one finds that

$$\begin{aligned} I(\mathbf{X}; W|\mathbf{Y}) &= H(\mathbf{X}|\mathbf{Y}) + H(W|\mathbf{Y}) - H(\mathbf{X}W|\mathbf{Y}) \\ &= H(\mathbf{X}|\mathbf{Y}) + H(W|\mathbf{Y}) - [H(\mathbf{X}|\mathbf{Y}) + H(W|\mathbf{X}\mathbf{Y})] \\ &= 0 , \end{aligned}$$

which concludes the proof that $I(\mathbf{X}; \mathbf{Y}) = 1$. Furthermore, following a procedure similar to those in the previous section, it can be shown that any ΦID that satisfies the axioms described above (partial ordering, non-negative

double-redundancy, and upper-bounded redundancy) correctly assigns 1 bit of information to $I_{\partial}^{\alpha \rightarrow \beta}$, and 0 to all other atoms.

Now that we have built these 16 single-atom systems, let us move to the integration measures of interest. For CD, ψ , and Φ^{WMS} , we will proceed by decomposing them in terms of ΦID atoms and checking whether each atom is positive (+), negative (-), or absent (0) from the decomposition to obtain the results in Table 1 of the article. Let us begin with CD, defined as the sum of transfer entropies from one variable to the other:

$$\begin{aligned} \text{CD} &= \frac{1}{2} \sum_{i=1}^2 I(X_i; Y_j | X_j) \\ &= \frac{1}{2} \sum_{i=1}^2 \left(I_{\partial}^{\{i\} \rightarrow \{1\}\{2\}} + I_{\partial}^{\{i\} \rightarrow \{j\}} + I_{\partial}^{\{12\} \rightarrow \{1\}\{2\}} + I_{\partial}^{\{12\} \rightarrow \{j\}} \right). \end{aligned} \quad (9)$$

Similarly, for ψ the atoms can be extracted from the decomposition of $\text{Syn}(X_1, X_2; Y_1 Y_2)$ in Eq. (4a):

$$\begin{aligned} \psi &= \text{Syn}(X_1, X_2; Y_1 Y_2) \\ &= I_{\partial}^{\{12\} \rightarrow \{1\}\{2\}} + I_{\partial}^{\{12\} \rightarrow \{1\}} + I_{\partial}^{\{12\} \rightarrow \{2\}} + I_{\partial}^{\{12\} \rightarrow \{12\}}. \end{aligned} \quad (10)$$

For Φ^{WMS} , the atoms can be extracted from the decomposition of Eq. (9) in the main text:

$$\Phi^{\text{WMS}} = -I_{\partial}^{\{1\}\{2\} \rightarrow \{1\}\{2\}} + I_{\partial}^{\{1\}\{2\} \rightarrow \{12\}} + \psi + \sum_{i=1}^2 \left(I_{\partial}^{\{i\} \rightarrow \{j\}} + I_{\partial}^{\{i\} \rightarrow \{12\}} \right). \quad (11)$$

The Φ_G case is slightly more involved, since it is not easily decomposable into a sum of ΦID atoms. According to the definition of Φ_G [14], for a system given by the joint probability distribution $p(\mathbf{X}, \mathbf{Y})$ one has

$$\Phi_G = \min_{q \in \mathcal{M}_G} D_{\text{KL}}(p \| q),$$

where \mathcal{M}_G is the manifold of probability distributions that satisfy the constraints

$$q(Y_i | \mathbf{X}) = q(Y_i | X_i). \quad (12)$$

Therefore, it suffices to check whether the probability distribution of the system satisfies the constraints in Eq. (12) — if it does, then $\Phi_G = 0$, and otherwise $\Phi_G > 0$ —, which can be easily verified for each system separately to obtain the Φ_G column in Table 1, concluding the proof.

VI. RESULTS OF SECTION ‘WHY WHOLE-MINUS-SUM Φ CAN BE NEGATIVE’

In this appendix we describe the details of the noisy autoregressive system and how to compute its ΦID to yield the results shown in Figure 5 of the main text.

Given the past state of the system x_t^1, x_t^2 , the next state is given by

$$\begin{aligned} x_{t+1}^1 &= a(x_t^1 + x_t^2) + \varepsilon_{t+1}^1 \\ x_{t+1}^2 &= a(x_t^1 + x_t^2) + \varepsilon_{t+1}^2, \end{aligned}$$

where $a = 0.4$ is a fixed coupling parameter and $\varepsilon_t^1, \varepsilon_t^2$ are zero-mean unit-variance white noise processes with correlation c . All information-theoretic functionals are computed with respect to the system’s stationary distribution, which can be shown to be a Gaussian and analytically calculated by means of a discrete Lyapunov equation [13, 15]. Once this distribution is obtained, the values of the atoms can be obtained following the procedures in Sec. III above.

VII. SIMULATION AND ANALYSIS OF WHOLE-BRAIN COMPUTATIONAL MODEL

To explore information decomposition in realistic neurophysiological data we study the Dynamic Mean-Field (DMF) model by Deco *et al.* [16, 17], which consists of a set of coupled differential equations modelling the average activity of

TABLE I. Dynamic Mean Field (DMF) model parameters

<i>Parameter</i>	<i>Symbol</i>	<i>Value</i>
External current	I_0	0.382 nA
Excitatory scaling factor for I_0	W_E	1
Inhibitory scaling factor for I_0	W_I	0.7
Local excitatory recurrence	w_+	1.4
Excitatory synaptic coupling	J_{NMDA}	0.15 nA
Threshold for $F(I_n^{(E)})$	$I_{\text{thr}}^{(E)}$	0.403 nA
Threshold for $F(I_n^{(I)})$	$I_{\text{thr}}^{(I)}$	0.288 nA
Gain factor of $F(I_n^{(E)})$	g_E	310 nC ⁻¹
Gain factor of $F(I_n^{(I)})$	g_I	615 nC ⁻¹
Shape of $F(I_n^{(E)})$ around $I_{\text{thr}}^{(E)}$	d_E	0.16 s
Shape of $F(I_n^{(I)})$ around $I_{\text{thr}}^{(I)}$	d_I	0.087 s
Excitatory kinetic parameter	γ	0.641
Amplitude of uncorrelated Gaussian noise v_n	σ	0.01 nA
Time constant of NMDA	τ_{NMDA}	100 ms
Time constant of GABA	τ_{GABA}	10 ms

multiple interacting brain regions. These equations represent each brain region as two reciprocally coupled neuronal populations, one excitatory and one inhibitory, with the corresponding synaptic currents $I^{(E)}$ and $I^{(I)}$ are mediated by NMDA and GABA_A receptors respectively. Different brain regions are coupled via their excitatory populations only, and the structural connectivity is given by the matrix C . The structural connectivity matrix was obtained from the HCP 900 subjects data release [18, 19], and was preprocessed in the same way as in Ref. [20], resulting in an 83×83 connectivity matrix corresponding to the Lausanne-83 brain parcellation [21]. For all other aspects of model configuration and simulation we follow Herzog *et al.* [22], and reproduce all relevant details here for convenience.

The full model is given by

$$\begin{aligned}
I_j^{(E)} &= W_E I_0 + w_+ J_{\text{NMDA}} S_j^{(E)} + G J_{\text{NMDA}} \sum_{k=1}^N C_{jk} S_k^{(E)} - J_j^{\text{FIC}} S_j^{(I)} \\
I_j^{(I)} &= W_I I_0 + J_{\text{NMDA}} S_j^{(E)} - S_j^{(I)} \\
r_j^{(E)} &= F\left(I_j^{(E)}\right) = \frac{g_E \left(I_j^{(E)} - I_{\text{thr}}^{(E)}\right)}{1 - \exp\left(-d_E g_E \left(I_j^{(E)} - I_{\text{thr}}^{(E)}\right)\right)} \\
r_j^{(I)} &= F\left(I_j^{(I)}\right) = \frac{g_I \left(I_j^{(I)} - I_{\text{thr}}^{(I)}\right)}{1 - \exp\left(-d_I g_I \left(I_j^{(I)} - I_{\text{thr}}^{(I)}\right)\right)} \\
\frac{dS_j^{(E)}(t)}{dt} &= -\frac{S_j^{(E)}}{\tau_{\text{NMDA}}} + \left(1 - S_j^{(E)}\right) \gamma r_j^{(E)} + \sigma v_j(t) \\
\frac{dS_j^{(I)}(t)}{dt} &= -\frac{S_j^{(I)}}{\tau_{\text{GABA}}} + r_j^{(I)} + \sigma v_j(t)
\end{aligned}$$

Above, j, k are indices that run across all N brain regions; F is the F - I curve relating input current to output firing rate of a neural population; J^{FIC} is the feedback inhibitory control parameter, optimised to yield average firing rates of approximately 3 Hz; and the sub- and superscripts E/I denote excitatory/inhibitory quantities, respectively. The model was simulated using a standard Euler-Maruyama integration method [23], using the parameter values shown in Table I. Note that all parameter values are fixed except the global coupling G , which we vary across simulations. Finally, the distributions of the simulated BOLD signals are approximated via Gaussian distributions, and the procedures in Sec. III above are applied to obtain the values of all Φ ID atoms.

VIII. NUMERICAL RESULTS REPLICATED WITH ALTERNATIVE Φ ID MEASURES

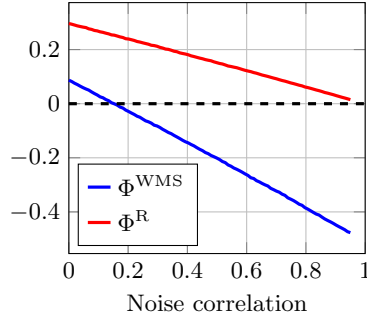


FIG. 1. Results in two-node AR system replicated with MMI double-redundancy.

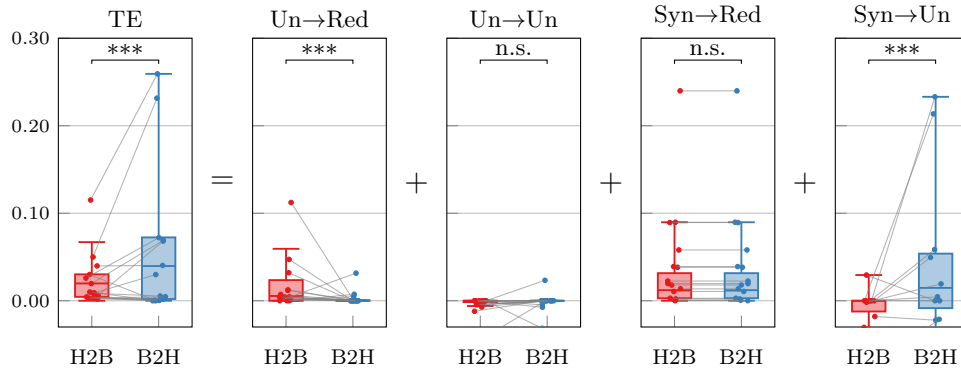


FIG. 2. Results in Fantasia dataset replicated with MMI double-redundancy.

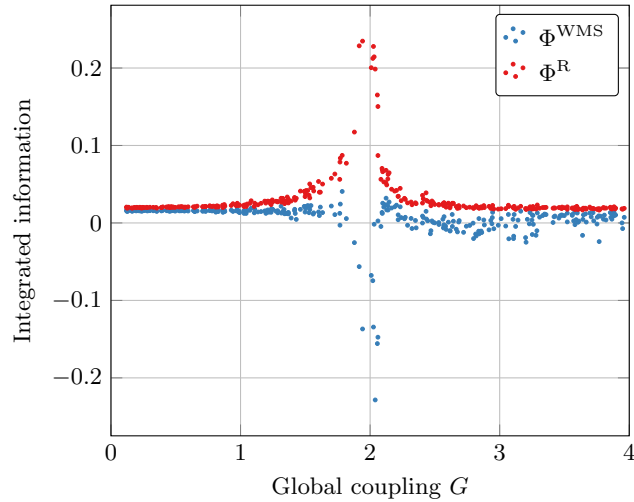


FIG. 3. Results in DMF whole-brain simulation replicated with MMI double-redundancy.

[1] C. A. Charalambides, *Enumerative Combinatorics* (Chapman and Hall/CRC, 2002).

- [2] P. L. Williams and R. D. Beer, Nonnegative decomposition of multivariate information (2010), arXiv:1004.2515 [cs.IT].
- [3] J. Crampton and G. Loizou, The completion of a poset in a lattice of antichains, *International Mathematical Journal* **1**, 223 (2001).
- [4] R. G. James, J. Emenheiser, and J. P. Crutchfield, Unique information via dependency constraints, *Journal of Physics A: Mathematical and Theoretical* **52**, 014002 (2018).
- [5] R. Quax, O. Har-Shemesh, and P. Sloot, Quantifying synergistic information using intermediate stochastic variables, *Entropy* **19**, 85 (2017).
- [6] F. E. Rosas, P. A. Mediano, B. Rassouli, and A. B. Barrett, An operational information decomposition via synergistic disclosure, *Journal of Physics A: Mathematical and Theoretical* **53**, 485001 (2020).
- [7] R. A. A. Ince, Measuring multivariate redundant information with pointwise common change in surprisal, *Entropy* **19**, 10.3390/e19070318 (2017).
- [8] For the rationale behind and extended discussion of local information measures see Lizier [24].
- [9] Equivalently, $f(\alpha, \beta)$ represents the length of the shortest path in the product lattice between the node $\alpha \rightarrow \beta$ and the lowest node.
- [10] F. E. Rosas, P. A. Mediano, M. Gastpar, and H. J. Jensen, Quantifying high-order interdependencies via multivariate extensions of the mutual information, *Physical Review E* **100**, 032305 (2019).
- [11] A. B. Barrett, Exploration of synergistic and redundant information sharing in static and dynamical gaussian systems, *Phys. Rev. E* **91**, 052802 (2015).
- [12] F. Rosas, V. Ntranos, C. Ellison, S. Pollin, and M. Verhelst, Understanding interdependency through complex information sharing, *Entropy* **18**, 38 (2016).
- [13] P. Mediano, A. Seth, and A. Barrett, Measuring integrated information: Comparison of candidate measures in theory and simulation, *Entropy* **21**, 17 (2019).
- [14] M. Oizumi, N. Tsuchiya, and S.-i. Amari, Unified framework for information integration based on information geometry, *Proceedings of the National Academy of Sciences* **113**, 14817 (2016).
- [15] A. B. Barrett and A. K. Seth, Practical measures of integrated information for time-series data, *PLoS Computational Biology* **7**, 1 (2011).
- [16] G. Deco, A. Ponce-Alvarez, P. Hagmann, G. L. Romani, D. Mantini, and M. Corbetta, How local excitation-inhibition ratio impacts the whole brain dynamics, *Journal of Neuroscience* **34**, 7886 (2014).
- [17] G. Deco, J. Cruzat, J. Cabral, G. M. Knudsen, R. L. Carhart-Harris, P. C. Whybrow, N. K. Logothetis, and M. L. Kringelbach, Whole-brain multimodal neuroimaging model using serotonin receptor maps explains non-linear functional effects of LSD, *Current Biology* , 1 (2018).
- [18] D. C. Van Essen, S. M. Smith, D. M. Barch, T. E. Behrens, E. Yacoub, K. Ugurbil, W.-M. H. Consortium, *et al.*, The WU-Minn Human Connectome Project: An overview, *NeuroImage* **80**, 62 (2013).
- [19] M. F. Glasser, S. N. Sotiropoulos, J. A. Wilson, T. S. Coalson, B. Fischl, J. L. Andersson, J. Xu, S. Jbabdi, M. Webster, J. R. Polimeni, *et al.*, The minimal preprocessing pipelines for the Human Connectome Project, *NeuroImage* **80**, 105 (2013).
- [20] A. I. Luppi and E. A. Stamatakis, Combining network topology and information theory to construct representative brain networks, *Network Neuroscience* **1**, 1 (2020).
- [21] L. Cammoun, X. Gigandet, D. Meskaldji, J. P. Thiran, O. Sporns, K. Q. Do, P. Maeder, R. Meuli, and P. Hagmann, Mapping the human connectome at multiple scales with diffusion spectrum MRI, *Journal of Neuroscience Methods* **203**, 386 (2012).
- [22] R. Herzog, P. A. Mediano, F. E. Rosas, R. Carhart-Harris, Y. Sanz, E. Tagliazucchi, and R. Cofré, A mechanistic model of the neural entropy increase elicited by psychedelic drugs, *Scientific Reports* **10** (2020).
- [23] P. E. Kloeden and E. Platen, *Numerical Solution of Stochastic Differential Equations*, Vol. 23 (Springer, 2013).
- [24] J. Lizier, *The Local Information Dynamics of Distributed Computation in Complex Systems*, Ph.D. thesis, University of Sydney (2010).